AN ABSTRACT OF THE THESIS OF

Brian K. Fuchs for the degree of Master of Science in Chemical Engineering presented on June 12, 2015.

Title: Immobilization of *Methylosinus trichosporium* OB3b in a Biolamina Plate Reactor for the Oxidation of Methane to Methanol

Abstract approved: _____

Karl F. Schilke

Methane is a flammable gas that is the main component of natural gas. It is a highly potent greenhouse gas, and accounts for about 20% of greenhouse gas emissions. Methane is routinely flared in many industrial processes without harnessing any of its energy. The environmental impact and wasted energy potential make it highly desirable to find an economically feasible process to use this methane.

One possibility is to convert methane into liquid fuels for transportation and energy generation. Current technologies to convert methane gas to liquid fuels (GTL) are complex, and the facilities are only economical at huge scales. Methane gas is very difficult to transport and store, so GTL plants must be located at the source of the methane, typically at large petroleum fields or refineries.

Biological conversion of methane to liquid fuels is an attractive alternative to traditional GTL processes, as microbial oxidation of methane can produce liquid fuels (e.g. methanol) at ambient temperatures and pressures. When biological organisms are combined with microfluidic technologies, which provide enhanced mass and heat transfer along with a high degree of process control, a very efficient conversion process can be attained at much smaller scales. A further advantage of microfluidics is that the reactors are inherently modular, allowing them to be adapted to practically any required size. This enables the economical conversion of small or remote methane streams to liquid fuels.

In this thesis, techniques are described for the immobilization of *Methylosinus trichosporium* OB3b in a biolamina-plate microreactor (BLP) for conversion of methane to methanol. Effective immobilization requires that the cells remain viable and immobile in the reactor, and that the encapsulation medium is stable and does not degrade during reactor operation. Calcium alginate gels were identified as an ideal immobilization medium, as they are inexpensive, non-toxic, and widely used for the immobilization of cells. Three main requirements must be met in immobilization of cells in the alginate: gel cohesion, gel adhesion, and cell viability. The alginate gel must remain cohesive throughout the entire reactor process, without substantial swelling, disintegration or degradation. The alginate must also adhere stably to the reactor surface, to prevent sloughing which may cause clogging and loss of biological activity. The immobilized cells also must remain metabolically active over the duration of the reactor run. Stable, thin (300-μm) calcium alginate films were achieved by combining an "internal gelation" process to uniformly cross-link the hydrogel, electrostatic adhesion of alginate gel on stainless steel reactor plates modified with aminopropyl-trimethoxysilane (APTMS), and buffering using 4-(2-hydroxyethyl)-1-piperazineethanesulfonic acid (HEPES) to minimize chelation of stabilizing calcium ions from the gel. The alginate-encapsulated *OB3b* cells retain viability and metabolic activity in these films, although their metabolism of methane to methanol appears to be slower

than pelagic cells. Overall encapsulation of *OB3b* in calcium alginate films is an effective method for immobilization, although further optimization is necessary.

Immobilization of *Methylosinus trichosporium* OB3b in a Biolamina Plate Reactor for the Oxidation of Methane to Methanol

by

Brian K. Fuchs

A THESIS

submitted to

Oregon State University

in partial fulfillment of
the requirements for the
degree of

Master of Science

Presented June 12, 2015

Commencement June 2016

Master of Science thesis of Brian K. Fuchs presented on June 12, 2015

APPROVED:

Major Professor, representing Chemical Engineering

Head of the School of Chemical, Biological and Environmental Engineering

---

Dean of the Graduate School

I understand that my thesis will become part of the permanent collection of Oregon State University libraries. My signature below authorizes release of my thesis to any reader upon request.

Brian K Fuchs, Author

ACKNOWLEDGEMENTS

This was a highly collaborative project with many people assisting to perform the required tasks. Dr. Karl Schilke advised me on this project and helped edit the manuscript. Eric Hobson worked with me throughout much of the project and helped develop the internal gelation protocol and also performed many of the live/dead staining experiments. Tanner Bushnell maintained the chemostats that grow the OB3b cells. Tanner also did most of the Gas Chromatography data analysis. Yorick Wahaus was in charge of the BLP reactor assembly and its operation. Dr. Anne Taylor performed many metabolic studies on the OB3b and did the research that led us to use cyclopropanol as an inhibitor. Anne also grew up the original OB3b culture that was used in these experiments. Paige Molzahn performed experiments on cell activity in the gel and also helped me harvest cells on numerous occasions. She also helped develop the method for the gel swelling experiments. Chris Loeb helped me design the flow cells and cut the PEEK lamina used in them. Malachi Bunn assisted with the CNC machining of the polycarbonate flow cells. Uranbileg Daalkhaijav (Ugi) performed the rheology experiments. Dr. Goran Jovanovic, Dr. Lew Semprini, and Dr. Mark Dolan all provided leadership on the project along with Dr. Schilke in order to meet the goals of the project. Dr. Dolan further assisted me with identifying and interpreting metabolic data.

TABLE OF CONTENTS

TABLE OF CONTENTS (continued)

TABLE OF CONTENTS (continued)

LIST OF FIGURES

Figure Page

LIST OF FIGURES (continued)

Figure Page

LIST OF FIGURES (continued)

Figure Page

LIST OF APPENDIX FIGURES

Immobilization of *Methylosinus trichosporium* OB3b in a Biolamina Plate Reactor for the Oxidation of Methane to Methanol.

Chapter 1

Introduction and Literature Review

Methane is a clear, colorless, and highly flammable gas that is the main component in natural gas. It is produced through a number of natural and industrial processes. As a greenhouse gas, methane is capable of trapping 25 times the amount of heat as CO_2 on an equivalent mass basis.[1] Furthermore, methane emissions are estimated to contribute about 20% of total greenhouse gas emissions and are the second largest promoter of global warming after CO_2.[2] Anthropogenic sources of methane currently account for about 63% of methane emissions per year.[3] The major sources of these emissions includes agricultural livestock, petroleum product mining and refining, and industrial sources and landfills. A breakdown of these sources can be seen in figure 1.1.

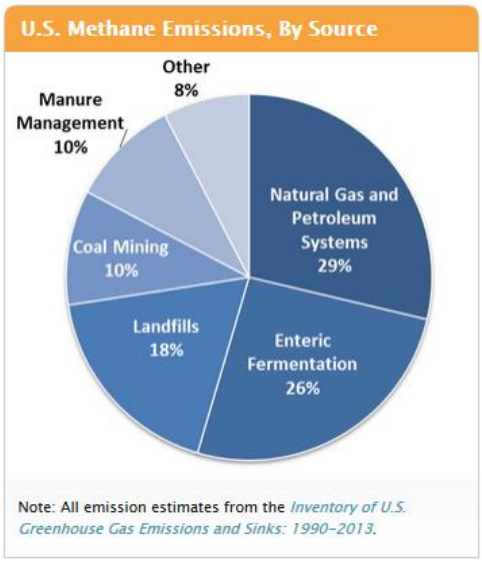

Figure 1. 1 - US methane emissions by source over the last 2 decades.[1]

Currently most of the methane created from these processes is either emitted into the atmosphere or flared without further energy generation. In fact, gas flaring in the acquisition of petroleum products alone accounted for 350 million tons of CO_2 emissions in 2013 and for nearly 1% of the total carbon emission that year.[4] This is the equivalent of the emissions of 770 million cars and results in 750 billion kWh of wasted energy.[4] These carbon emissions are unnecessary and methane flaring results in a huge amount of wasted energy.

Current advances in oil extraction and hydraulic fracturing have made methane in the form of natural gas more plentiful and readily available. These new sources of methane combined with wasted methane from flaring accounts for a significant supply of underutilized and wasted fuel. Given high methane availability, the extremely detrimental environmental effects of emitted methane, and the amount of energy currently wasted through methane flaring; it is highly desirable to find economically viable uses for methane.

One recent proposal is to utilize methane for similar uses to that of liquid petroleum products. Methane has not been utilized in this way on a large scale presently because of the difficulties and cost in transporting and storing it.[5] As a gas, methane has a low volumetric energy

density, which makes it inherently difficult to use as an automobile fuel source.[6] Furthermore, significant infrastructure would have to be constructed in order to make it viable as a transportation fuel. Liquefying or compressing methane has been considered to increase its volumetric energy density and make it easier to transport, however this process requires methane to be compressed to 20-25 MPa or cooled to -162 °C.[5] Compressing or cooling methane to these levels present significant costs and safety concerns which make it impractical.

Another proposed use for natural gas is to convert methane to other natural liquid fuels through gas to liquid (GTL) processes. The most common process produce these fuels is through conversion of methane to syngas and then to longer chain hydrocarbons using a Fischer-Tropsch process.[5] In the first step in this process, syngas is produced through partial oxidation of methane to CO and H_2, which is typically accomplished through steam reforming of the methane over a catalyst.[7,8] After this the Fischer-Tropsch process is implemented, which requires high temperatures and pressures along with numerous process steps.

Because of the number of process steps and heat and pressure changes, large scale production of fuels using this process requires large facilities and capital investment. Recent GTL plants constructed in Qatar required capital investments on the order of $18-20 billion.[9] In order to make these plants commercially viable, they must take advantage of economies of scale. These plants produce anywhere from 10,000 to 140,000 barrels of synthetic crude/day.[9] The size and cost of constructing plants this size make it economically infeasible to process smaller methane sources, so they can be implemented only at large petroleum fields.

Recently, attempts have been made to directly convert methane to methanol using catalysts. If successful this would eliminate many of the process steps required in Fischer-Tropsch processes and should considerably reduce the size of a GTL plant. Many different homogenous and heterogeneous catalysts have been tried in several different processes to accomplish this, but none have proven economically viable. [10,11,12] This route is challenging from

a chemistry standpoint because the C-H bonds of methane are fairly unreactive and the products of these catalytic reactions are more reactive than methane.[10] Because of this, yields and selectivity of the desired product are typically very low making all current direct conversion process economically unviable. [12]

Attempts have been made to reduce the size and cost of GTL plants. Both Shell and Velocys have produced modular GTL designs that can convert smaller amounts of natural gas to synthetic crude making them better suited for more remote methane sources.[9,13] These new modular technologies are significantly reduced in size and are suited for methane sources that can provide 200-5000 barrels of synthetic crude/day.[9] These modular reactors are significantly smaller and can target smaller and more remote methane sources, however they are still of a scale that makes them viable only for oil fields and oil production, and not other smaller methane sources such as landfills.

A number of reviews have been recently published on the possibility of using biological approaches for GTL conversion (bio-GTL).[3,5,6,14] Bio-GTL processes use cells or enzymes as a biocatalysts to convert methane sources to liquid fuels. A number of cell candidates have been identified for potential use in these technologies including methanotrophs, ammonia oxidizing bacteria, and methane oxidizing archea.[5] Bio-GTL looks very promising because it requires much milder temperatures and pressures and fewer process steps than Fischer-Tropsch processes.[6] This results in a significantly lower process cost and smaller plant sizes, which makes more remote methane sources more accessible to these technologies.

Microreactor technologies can also be useful in reducing the size of GTL processes. Microreactors are defined as reactors in which the chemical reaction takes place in a vessel with at least one dimension less than 1mm. These reactors are characterized by high surface area to volume ratios, low diffusion lengths for reactants, and high heat transfer rates.[15,16] These advantages allow for high catalyst or biocatalyst loading and decreased diffusion lengths, which

can improve reaction efficiency and in many cases will allow for a reactor design that is limited by reaction kinetics. A further advantage of microreactors is that it is often easy to maintain laminar flow, allowing for a large degree of process control in the reactor. Microreactors can also often be designed to be modular. This simplifies scale up of microdevices as you can scale up simply by adding more modules.[17] These advantages of microreactors allow for miniaturization of chemical technologies which could be applied to GTL processes.

In this study, a microfluidic bioreactor was constructed in order to convert methane to methanol. This reactor takes advantage of both the process enhancements available in microreactors and the advantages of bioconversion of methane. The reactor was designed so that a number of flat plates with immobilized cells could be stacked on top of each other with a media solution and methane and oxygen gas bubbles flowing over the cells (see figures 1.2 and 1.3). The high surface area to volume ratio of this design allows for a high density of cells to be packed near the flow path of the media. Furthermore, methane and oxygen are fed into the reactor as bubbles. The gas-liquid interface of these bubbles is ~10 μm from the top of the film which allows for increased mass transfer of the gasses to the cells and keeps the media saturated with these components throughout the reactor. This is very important as methane and oxygen are only sparingly soluble in aqueous solutions, so maximizing their concentrations in the solution will increase methane turnover rates in the reactor. The large surface area of the reactor also allows for significant temperature control which is important for cellular metabolism. The stacked plate design allows for easy scaleup of the device by increasing the number of layers in the devices. This allows for reactors to be designed to appropriate sizes for various applications.

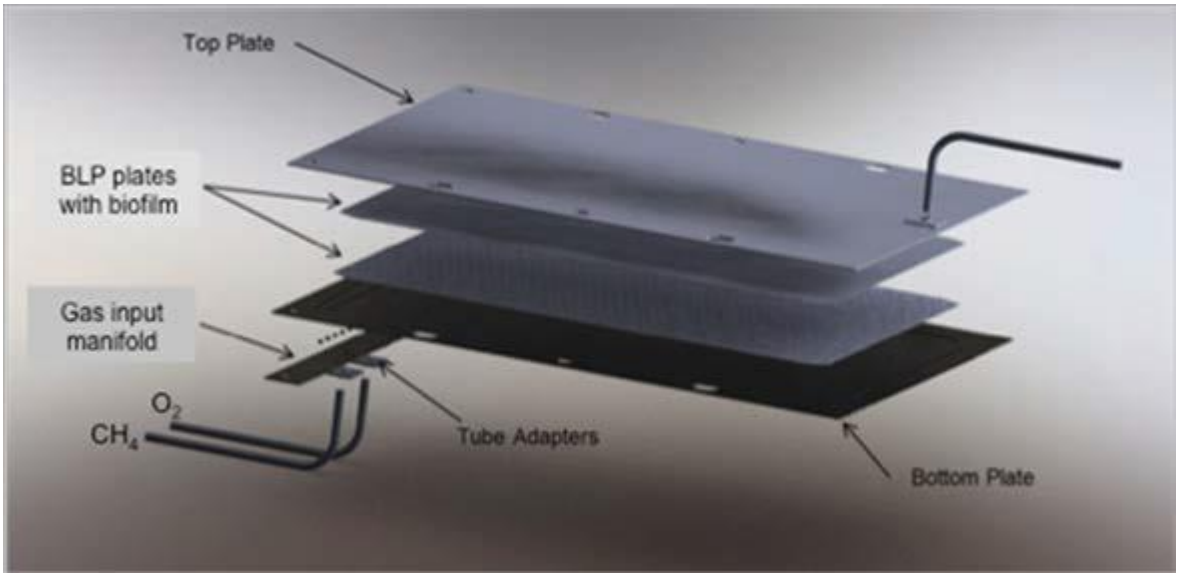

Figure 1. 2: Conceptual Design of Multiplate Microreactor.

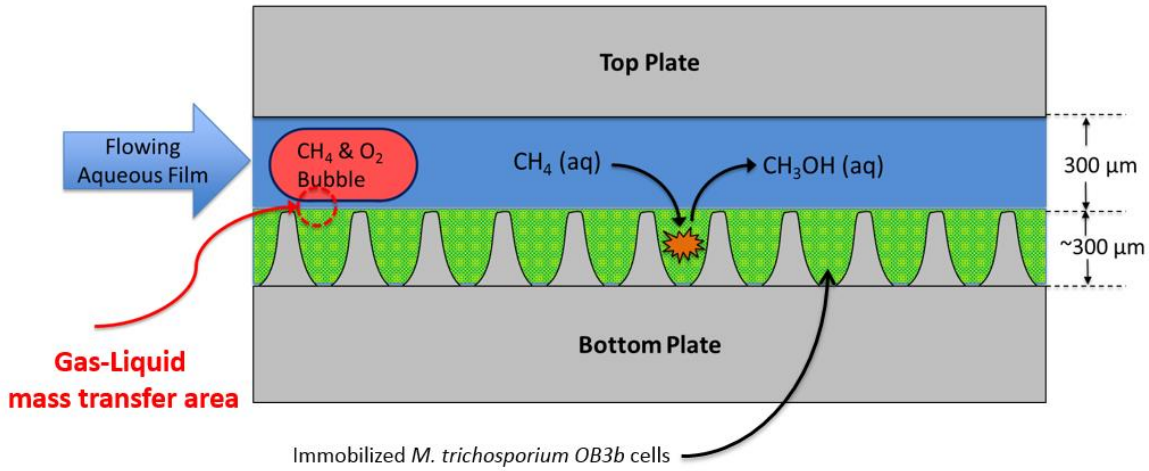

Figure 1. 3: A schematic of two phase flow in the BLP. Two phase flow with methane and oxygen bubbles in cell media are perfused through the reactor over cells immobilized in alginate in the bottom plate. The dimensions are designed to minimize diffusion paths so that a maximal amount of methane and oxygen can be fed to OB3b cells throughout the reactor.

Methylosinus trichosporium OB3b (referred to as "OB3b" from here on) was identified as a good cell candidate for use in this reactor system. OB3b is a methanotroph that is found in natural environments with high methane levels and low oxygen levels.[18] Methanotrophs are bacteria that utilize single carbon compounds for cellular metabolism. The metabolic scheme of methanotrophs can be seen in figure 1.4. In this process methanotrophs oxidize methane to

methanol using a methane monooxygenase (MMO) enzyme, and then oxidize it further methane into other metabolic products.

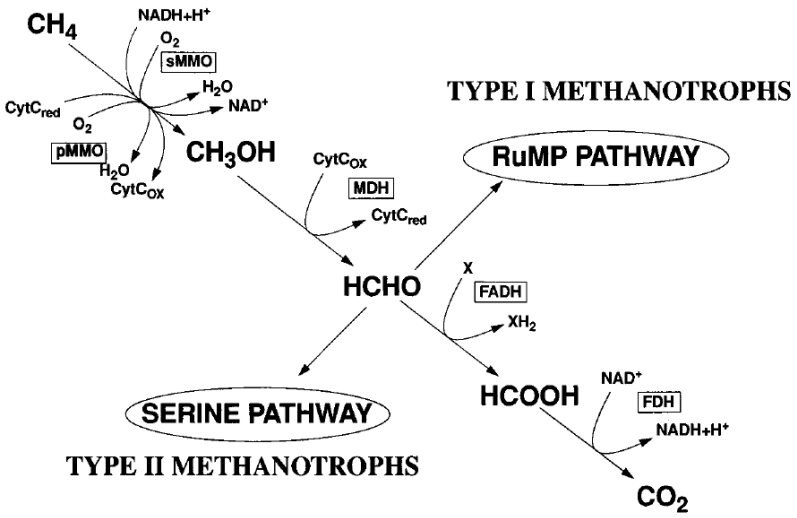

Figure 1. 4: The metabolic scheme of methanotrophic organisms.[18] For the production of methanol MDH activity must be inhibited without significant inhibition to MMO. Metabolism beyond methanol is important to cellular function in order to regenerate electrons used by the MMO.

For production of methanol using methanotrophs, there are two key enzymes to consider: MMO and methanol dehydrogenase (MDH). MMO catalyzes the oxidation of methane to methanol as shown in equation 1.1.[19] This oxidation is an energy consuming process that requires the use of two electrons. These electrons must be replenished through the oxidation of methanol to further metabolites.

$$CH_4 + O_2 + 2e^- + 2H^+ \rightarrow CH_3OH + H_2O \qquad \text{(Equation 1.1)}$$

There are two types of MMO that OB3b can express: soluble MMO (sMMO) and particulate MMO (pMMO). sMMO is found in the cytoplasm of the cell and is soluble in aqueous environments. It uses NADH as the electron source which is replenished in downstream metabolism when formic acid is oxidized to CO_2.[20] pMMO is an insoluble enzyme that is bound to the bacterial membrane. It is expressed when copper is present in the environment of OB3b which It as a cofactor at the active site to help with the oxidation of methane. The method by

which electrons are replenished using pMMO is still under debate,[21] but it likely has to do with electron transport interactions with other membrane bound complexes.

Methanol dehydrogenase oxidized methanol to formaldehyde which can be further oxidized to other metabolic products and cellular components. Inhibition of MDH is essential to prevent the consumption of methanol for use in these downstream products. Several MDH inhibitors have been researched in recent years, including: NaCl, HH_4Cl, EDTA, and cyclopropanol.[15,19] These inhibitors have shown varying degrees of success in different systems. Many MDH inhibitors also inhibit MMO and thus must be carefully administered in order to prevent loss of MMO activity.[19] In order to produce as much methanol as possible, the ratio of MDH inhibition to MMO inhibition must be maximized, while still getting appreciable MMO activity. This can be a hard balance to achieve.

In our system it was decided to make the OB3b express sMMO by removing all copper from the cell media. We desired sMMO expression because it has been shown that sMMO has a substantially higher activity than pMMO in systems with large amounts of dissolved methane (see figure 1.5).[23] The methane levels in the reactor are always high due to the perfusion of gaseous methane bubbles through it, so sMMO inclusion is likely to provide higher yields.

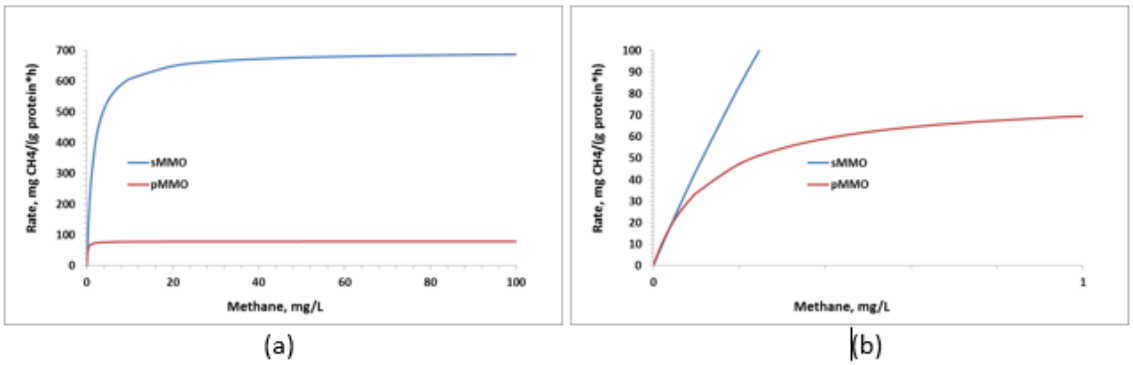

Figure 1. 5: Theoretical activity curves for methane utilization of sMMO and pMMO based off of the numbers from Lee et al.[23] Values for V_{max} and k_m were provided in the paper for both enzymes and Michaelis-Menten kinetics were applied. (a) Shows the MMO activities over a wide range of methane concentrations. (b) Shows the MMO activities at low methane concentrations. At very low methane concentration pMMO has a higher activity than sMMO, but sMMO starts to outperform pMMO at a methane concentration of ~0.2 mg/L (~10% of saturation at ATP)

Early experiments, performed by Dr. Anne Taylor, identified cyclopropanol as an effective inhibitor for our system. Cyclopropanol provided sufficient MDH inhibition in these tests while leaving MMO largely intact. However, complete inhibition of MDH with cyclopropanol prevents the cells from further metabolizing any of the methanol, which prevents the cell from replenishing NADH. Extended inhibition in this way leads to the starvation of the cells. One way to resolve this problem would be to feed the cells formate to allow them to complete their metabolism and replenish NADH. However this is not an economical solution since formate is a more expensive product than the methanol we are trying to produce. Another option is to pulse cyclopropanol through the reactor leading to temporary inhibition of sMMO. The cells can then replenish their MDH enzymes over time, which allows them to regenerate NADH and make other required metabolic products.

Immobilization of OB3b cells in the reactor is a vital aspect of the reactor design and function. Many immobilization mediums have been developed for effective immobilization of cells for various uses. Groboillot et al. immobilized lactic acid bacteria in chitosan for the use in milk acidification.[24] Glioma and hybridoma cells were immobilized in agarose for monoclonal antibody production by Cadic et al.[25] Muthukumarasamy et al. used alginate, κ-carrageenan and xanthan gum to protect probiotics from acidic conditions similar to the stomach.[26] Other immobilization mediums have been used in other applications as well to suit the needs of the system.

One of the most common mediums for immobilization is alginate. Alginate has been used to immobilize cells for a number of different situations. Some uses for alginate include: protecting cells as they pass through the GI tract,[22] protecting cells through cryopreservation processes,[27] and immobilizing hepatic cells in a bioreactor.[40]

Because alginate has been widely researched and is used in a number of immobilized cell technologies, it was identified as an ideal choice for the immobilization medium in the reactor system. Alginate is a naturally occurring long chain polysaccharide harvested from brown algae.[29] It is composed of two monomeric building blocks, β-D-mannuronic acid (M-blocks) and α-L-guluronic acid (g-blocks), structures of which can be seen in figure 1.6.[30] The ratio of these building blocks can have a significant effect on alginate structure and its viability as an immobilization medium.[40] When alginate solutions are exposed to divalent cations such as Ca^{2+} the alginate strands ionically crosslink forming a viscoelastic gel. This occurs because the Ca^{2+} has a higher affinity for the carboxylic groups in the alginate than the Na^{+} and thus displaces them. When two carboxylates from different strands connect to the same calcium ion, the strands become linked giving the gel structure. This forms an "egg box" structure in the alginate with the carboxylic groups in the alginate strands coming together as seen in figure 1.7 causing a gel to form.[31]

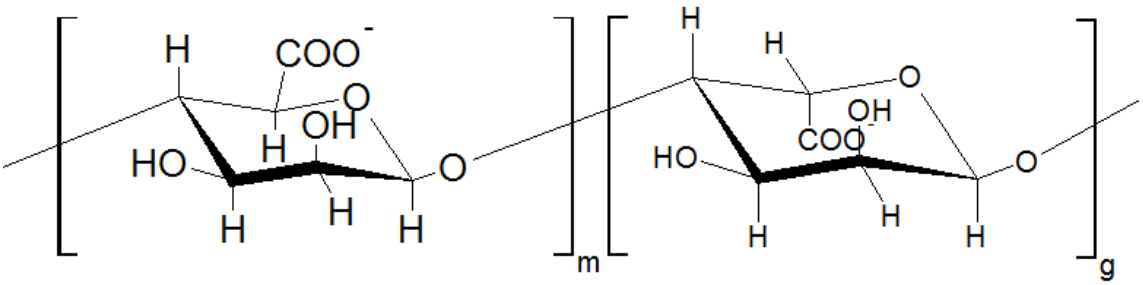

Figure 1. 6: Empirical sketch of alginate. Alginate is composed of strands of an interspersed combination of β-D-mannuronate (left) and α-L-Glucuronate (right). The carboxylates can bind monovalent ions such Na^{+} to form a viscous liquid or divalent ions such as Ca^{2+} to form a viscoelastic gel.

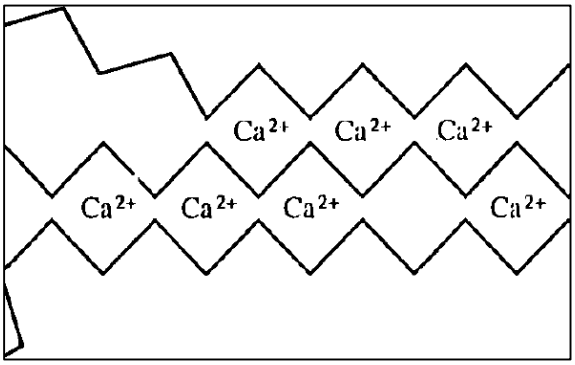

Figure 1. 7: "Egg box" structure of calcium alginate gels.[31] The Ca^{2+} ions brings the alginate strands together causing it to form a gel.

This study looks primarily at the encapsulation of OB3b cells in order to immobilize them in a BLP reactor. Immobilization in this reactor system is substantially different from immobilization in other bioreactor systems in that the BLP requires that the cell be immobilized in a thin alginate film. In the vast majority of other systems with alginate immobilized cells the cells were encapsulated in gel beads which do not need to adhere to a surface. Effective immobilization requires that the cells remain immobilized and alive in the reactor and requires that the immobilization medium does not degrade. In this study we have separated immobilization tasks into three distinct areas: cohesion of alginate gels, adhesion of alginate gels to the reactor, and immobilized cell viability and performance. Success in all three areas is vital for the proper operation of the BLP reactor.

Chapter 2

Alginate Cohesion

Introduction

The cohesiveness of the immobilization medium in the BLP reactor is of vital importance to its function. If the medium fails to remain cohesive the cells may no longer stay immobile in the reactor and washout. Furthermore, sloughing of the immobilization medium could lead to pieces of the medium being lodged in the reactor orifices and clogging them. The destruction of the immobilization medium could also cause flow maldistribution in the reactor causing problems in reactor operation.

Calcium alginate hydrogels are held together by the ionic crosslinking of calcium ions to the carboxylate groups on the alginate polymer. The most common paths for calcium alginate degradation in alginate is through displacement of these calcium ions in the gel structure. This in turn would cause the alginate strands to separate, leading to the alginate losing much of its strength.

There are several known causes of calcium loss in alginate hydrogels. A study by LeRoux et al. showed that alginate gels have significantly reduced equilibrium compressive and shear moduli when exposed to physiological relevant levels of NaCl indicating a loss of gel cohesiveness.[30] The loss of cohesiveness was attributed to competitive displacement of the calcium ions in the alginate by the sodium ions of the NaCl. Chelators such as EDTA and sodium citrate have been shown to completely dissolve alginate gels in high concentrations by chelating the calcium from its structure.[32,33] In lower concentrations, these chelators could significantly weaken an alginate gel without dissolving it. Phosphate has also been shown to chelate calcium out of alginate and form calcium-phosphate precipitates,[34] though to a lesser degree than EDTA and citrate. Alginate degradation has also been shown under acidic conditions.[35] Under acidic

conditions protons can competitively displace the calcium ions in the gel, forming alginic acid. Loss of calcium in the alginate from any of these sources can significantly weaken and degrade the gel.

Other forms of gel degradation may also occur in the reactor too. Shear stresses in the microreactor are not inconsequential and could contribute to gel degradation over time. Because the depth of the flow path in the BLP is very small, higher shear stresses may be applied to the alginate surface than would be found in other fluidic systems. Furthermore, the addition of gas bubbles in the reactor could produce high local shear forces on the gel. This extra shear may be enough to degrade the gel. Also if the bubbles were to enter or contact the gel itself the surface tension on these bubbles may provide enough force to tear the gel apart.

The conditions of the gel formation process also can affect the mechanical stability of the gel. In most systems, alginate beads are formed by extruding alginate droplets from a needle into a calcium chloride solution. Submersion of alginate films in calcium chloride solutions can also be used to make alginate gels in different geometries. Alginate films made in this way show denser crosslinking in the first 50 μm near the surface of the gel than further into the gel.[40] This indicates that the gel is stronger at its surface than in its the deeper layers.

Another method of alginate gel formation is to slowly solubilize a calcium source inside the gel, causing the gel to form homogenously throughout the gel. Kuo and Ma made gels in this way by adding glucono-δ-lactone (GDL) and calcium carbonate to alginate.[36] Calcium carbonate is sparingly soluble in water and the alginate and cannot access the calcium as a crosslinking agent. Hydrolysis of glucono-δ-lactone produces gluconic acid causes local pH drops which allows the release of calcium ions from the calcium carbonate, making them accessible to the alginate as a crosslinker as seen in figure 2.1. This method forms homogenous crosslinking throughout the gel volume.[36] This method can be advantageous as it adds uniform crosslinking

strength throughout the entire gel and not just at the surface. Furthermore, it makes gels of various shapes easy to make.

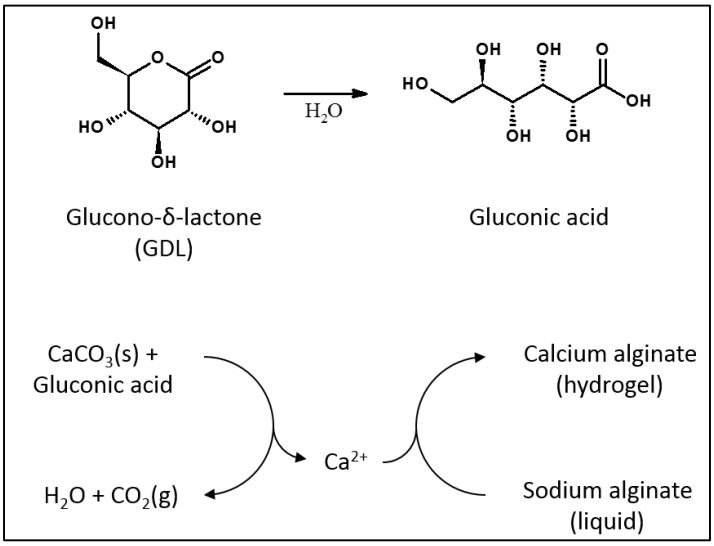

Figure 2. 1: Solubilization of Ca^{2+} from calcium carbonate by glucono-δ-lactone (GDL). The GDL can strip the Ca^{2+} from the calcium carbonate which is normally insoluble. The Ca^{2+} is then accessible to the alginate as a crosslinking agent.

In this chapter, the cohesiveness of alginate hydrogels under flow condition in the BLP is investigated. Methods for crosslinking the gel both internally and externally were developed. The effects of the media components on the gel films are also investigated. Tests both in the BLP and in other flow systems were peformed in order to elucidate the effects of media components on the gel films and to help determine the optimal media composition for gel integrity.

Materials and Methods

Sodium Alginate Solution Preparation

Medium viscosity sodium alginate powder was purchased from Sigma-Aldrich (SIGMA #: A2003). 1 L of 4 wt% alginate solution was made by adding 40 g alginate powder to a bottle. The powder was then wetted slightly with ethanol to help the alginate dissolve. 1 L of RO water was then added and the alginate solution was stirred while the water was being added. The alginate was then put on a stir plate and with a stir bar in it to agitate it. Occasionally, alginate

clumps were broken up mechanically with a glass rod or by shaking the solution with the stir bar in it. If necessary the alginate was heated to 50 °C to decrease the viscosity and increase the alginate solubility. After all the alginate powder dissolved, the alginate was autoclaved for 40 minutes at 110 °C for sterilization.

Internal Gelation of Sodium Alginate

4 wt% sodium alginate was prepared as described above. 1 M solutions/suspensions of glucono-δ-lactone (GDL) and calcium carbonate were prepared by adding the appropriate amount of GDL or calcium carbonate to RO water. (note: calcium carbonate does not actually dissolve in this suspension). After thoroughly mixing the $CaCO_3$ solution, an appropriate amount of the $CaCO_3$ suspension was added to the 4 wt% alginate solution to obtain a final $CaCO_3$ concentration of 0.04 M. An appropriate amount of 1 M GLD solution was added to an equivalent volume of RO as the alginate to obtain a final GDL concentration of 0.08 M. The two solutions were then combined and stirred vigorously for 30 seconds. The solutions are then ready to be poured into a desired shape to set. The solution will start nucleating in 2.5-5 minutes and normally fully sets within 20 minutes. This creates a solid 2 wt% alginate gel. Additional submersion in a $CaCl_2$ solution can provide additional gel strength.

Flow Cell Manufacturing and Experiments

Manufacturing

A stacked drawing of a flow cell can be seen in figure 2.2. Full schematics of these cells can be seen in Appendix A. Pieces of 3/8” thick and 1/2” thick impact resistant polycarbonate (PC) purchased from McMaster-Carr (item #: 1749K639 and 1749K649) were cut into 4” x 7” rectangles. A 50 mm x 75 mm x 500 µm well was cut into the center of the 3/8” thick piece using a CNC mill in order to provide a place for alginate deposition in the flow cell. Screw holes (1/4”) were also cut on both pieces using a CNC. Pieces of 250 µm thick polyetheretherketone (PEEK)

were cut out into 4” x 7” rectangles with matching screw holes to the PC pieces using an ESI 533 Laser Cutter located at the Microproducts Breakthrough Institute located in Corvallis. A rhomboidal flow path was also cut into the middle of the PEEK pieces using the laser cutter. Inlet and outlet holes were tapped into the ½” thick PC near the inlet and outlet tips of the flow path (inlet: size 10-32 for IDEX F-330B fitting, outlet: size ¼-28 for IDEX LT-115).

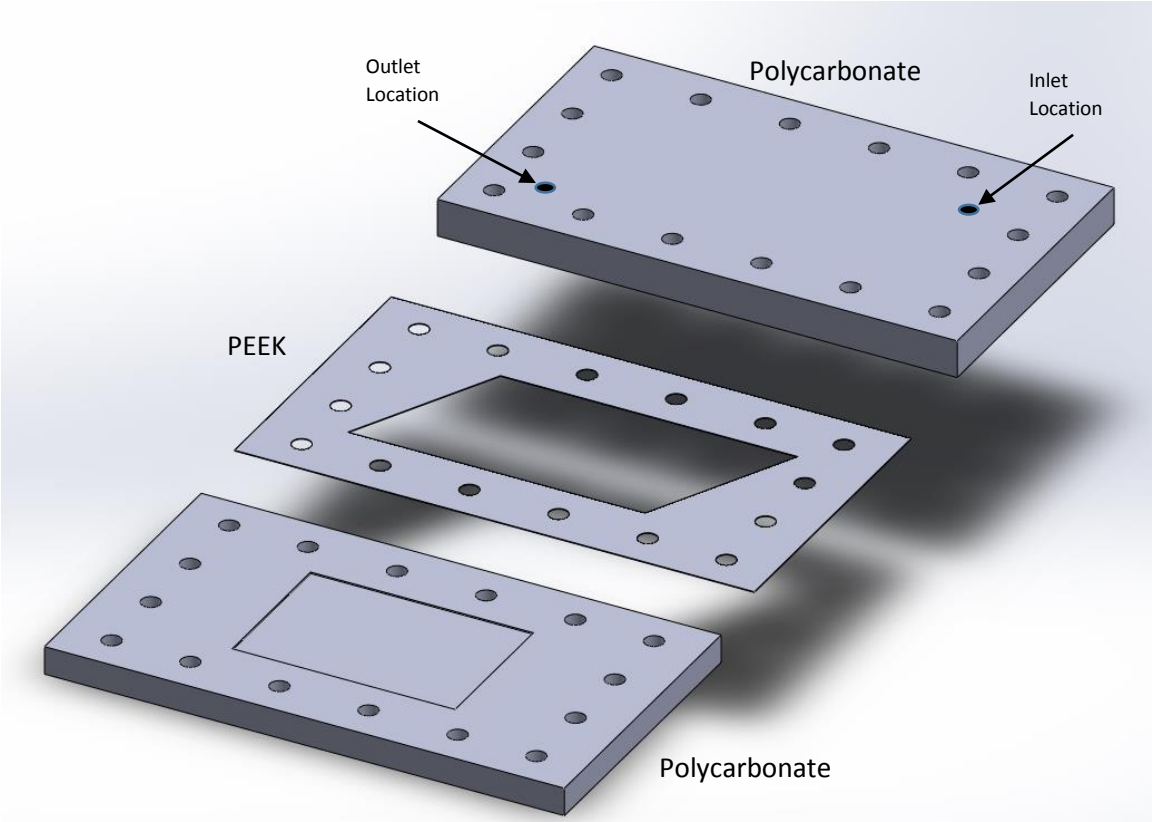

Figure 2. 2: SolidWorks drawings of microfluidic flow cells. Top and bottom pieces were machined out of polycarbonate with a CNC mill. The middle piece was made out of PEEK cut by a ESI 533 Laser Cutter. Alginate gels were deposited in the well of the bottom piece and the device was assembled with two PEEK middle pieces sandwiched between the polycarbonate top and bottom pieces and held together with screws. The PEEK pieces create a flow path for media solutions in the device. Inlet and outlet ports were tapped into the top piece to allow flow through the device. For dimensions see Appendix A.

Polycarbonate Silanization for Flow Cells

Flow cells were constructed as previously described. The flow cell base was cleaned in 200 proof ethanol for 10 minutes on a shake plate. A 246:3:1 solution of 200 proof ethanol, water,

and APTMS (Lot #: BCBL6126V) was made. The wells in the flow cell base plates were filled with the solution in order to only silanize the well. Because the solution evaporated quickly, more solution was added to the wells every 10 minutes. After 2 hours the solution was removed from the well and any excess solution was washed off with 95% ethanol. The silane coated PC pieces were cured @ 125 °C for 2 hrs to dehydrate the siloxane bonds. Another layer of APTMS was deposited using the same solution recipe and method. The pieces were cured again for 2 hrs at 125 °C and washed in ethanol twice for 10 min. Background on APTMS coatings can be found in the chapter 3 introduction.

Flow Cell Assembly

A gel layer was deposited in the well of the flow cell using the internal gelation protocol. The alginate was scraped flush with the top of the well using a Teflon rod to make a gel layer the same height as the rest of the bottom flow cell piece. Once the alginate had set the piece was submerged in a 0.1M $CaCl_2$ solution for 30 minutes. The device was then assembled using 1–¼" long 1/4" diameter stainless steel bolts with matching washers and nuts. Two PEEK pieces were sandwiched between the two polycarbonate layers and the bolts were tightened to a torque of 40 in-lbs to make a 500 µm liquid flow path. 1/16" OD tubing was attached to the inlet port (IDEX F-330B) and 1/8" OD tubing was attached to the outlet ports (IDEX LT-115). The inlet tubing was attached to Cole Palmer L/S 13 tubing (Cole Palmer # 96410-13) which was attached to a peristaltic pump. The inlet and outlet ports were screwed into the inlet and outlet taps until finger tight.

Flow Cell Experiments

One L of deionized water, phosphate media solution, HEPES media solution, or water acidified with HCl to a pH of 4 were prepared for each experiment (recipes of media solutions can be found in appendix C). The inlet and outlet tubes of 3 flow cells were placed in a solution

bottle so that the solution was cycled through the flow cells and all flow cells were connected to the same basin. A picture of the setup can be seen in figure 2.3. Media was perfused through the flow cells at a rate of 5 mL per minute to approximate the fluid velocity of ~ 20 cm/minute in the original BLP reactor proposal. After 18 hours of perfusion the flow cells were taken apart and swelling and rheological studies were performed.

Figure 2. 3: Picture of the experimental flow cell setup. Media is cycled through the flow cells in order to determine the effects of cell media on the alginate. Depth testing and rheological studies were then be performed.

Swelling Studies

Swelling studies were performed in order to determine the effects of different media compositions and solution conditions on alginate films. The swelling of alginate gels in the flow cell was measured after 18 hours of operation. A flow cell base plate with alginate was submerged in a water bath on a stand (see figure 2.4). The microscope was positioned looking over the top surface of the flow cell, so that only gel above the surface can be seen. A needle was loaded onto a stand that has a step control that can lower the needle 10 μm at a time. In early experiments (flow cells perfused with DI water and acidic water), the needle was positioned right

above the alginate on the slide. The needle was then lowered through the alginate in 10 µm increments while counting each increment until the tip of the needle disappeared below the top edge of the alginate well and the number of steps to get to this point was reported. In later experiments (flow cells perfused with phosphate and HEPES media), the needle was lowered into the well until it hit the bottom of it and it stopped moving. The needle was then raised in 10 µm increments until it was fully out of the gel. If the gel clung to the needle as it was pulled out and then relaxed, then the needle was lowered 10 µm at a time and the number of steps back to the resting gel was subtracted from the number of steps it took to pull the needle from the gel. A further 50 steps were subtracted from the total to account for the depth of the well. This change in procedure was made to prevent error if the microscope was not setup perfectly flush with the top face of the flow cell. Three locations were probed on each flow cell. One location was the highest point of the alginate on the cell, one location was the lowest point on the flow cell, and one was a point that was representative of the median level of the alginate. The amount of alginate swelling was then determined by multiplying the number of steps by 10 µm.

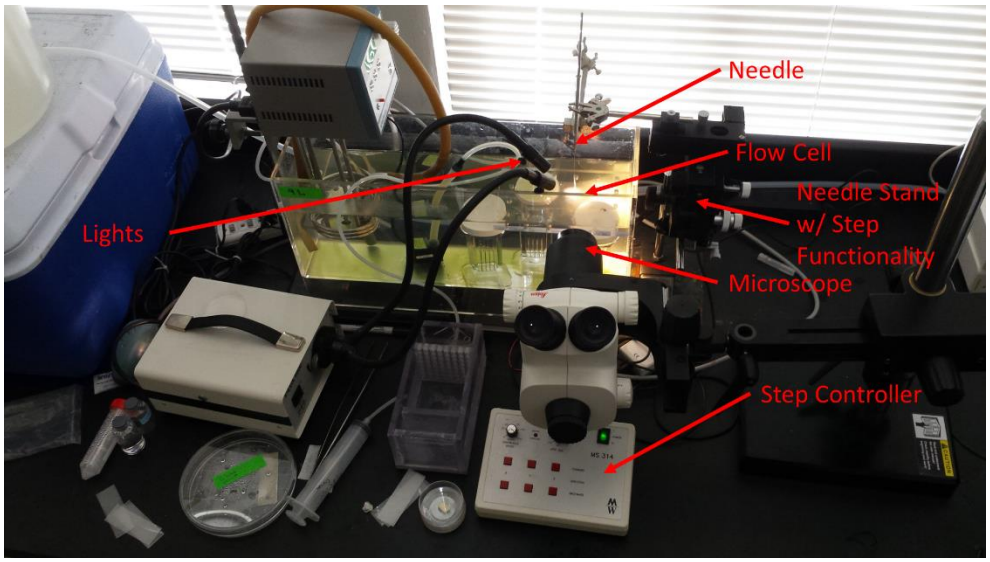

Figure 2. 4: Picture of the Microscope setup for swell testing. A needle was lowered in 10 μm increments through the gel using a step controlled in order to measure the gel depth proud of the surface of the flow cell. This indicates how much the gel swelled in the flow cells.

Rheological Studies

In order to get quantitative data on the cohesiveness of the alginate gels under various solution conditions, plate on plate oscillatory rheology was performed. Flow cells were operated as stated above with DI water and acidic water. The flow cells were taken apart and the base PC plate was removed and with the gel in it. The plate was then mounted to a DHR 3 rheometer. The setup had a 40mm stainless steel 0° geometry. An oscillation amplitude sweep was performed and it was determined that a 0.5 Hz oscillation amplitude was ideal for this system. A frequency sweep was then performed with angular frequencies between 0.1 and 100 rad/s and a strain of 0.05%. Bulk modulus data was then plotted against the angular frequency.

BLP Assembly and Operation

Gel Loading

Cells were obtained from the chemostat that Tanner Bushnell maintained (concentration varied). The cells were spun down and resuspended in 15 mL of water. Internal gelation protocol (see above) was then followed to get a mixture of alginate and cells that would set. Before the alginate solidified, it was poured into one side of the reactor bottom plate. A Teflon rod 1”thick was immediately used to scrape the alginate mixture across the plate and make it flush with the top of the reactor. The plate was then set out for 15 minutes for the alginate to set. After the alginate set the plate was submerged in 0.1 M calcium chloride to allow the alginate to crosslink further. After 10 minutes the plate was removed and any excess alginate on the sides of the reactor and the O-ring grooves was removed with a razor. The plate was then placed back into the calcium chloride solution for a total submersion time of 1hr.

BLP Assembly

A flow diagram of the reactor experimental process can be seen in figure 2.5. Pictures of the reactor flow and bottom plate can be seen in figures 2.6 and 2.7. The top plate was treated

with a 1% F-127 solution prior to an experiment to make it more hydrophilic. The reactor plates were attached to the appropriate clamp plates and then these plates were aligned and assembled with bolts to 15 ft-lbs (see figure 2.8). The plate was then inserted into the reactor box that was plumbed with flow controllers and pressure gauges as seen in figure 2.9. The gas and liquid fittings were then assembled with the liquid fittings connected to an HPLC pump and the gas fittings attached to compressed air and methane canisters (after going through gauges and control valves).

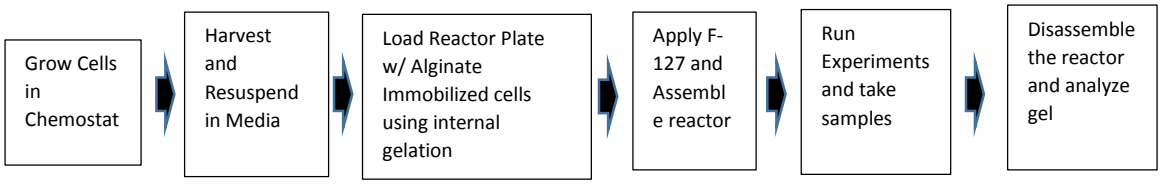

Figure 2. 5: Flow diagram of the reactor experimental process.

Figure 2. 6: Picture of the reactor flow plate.

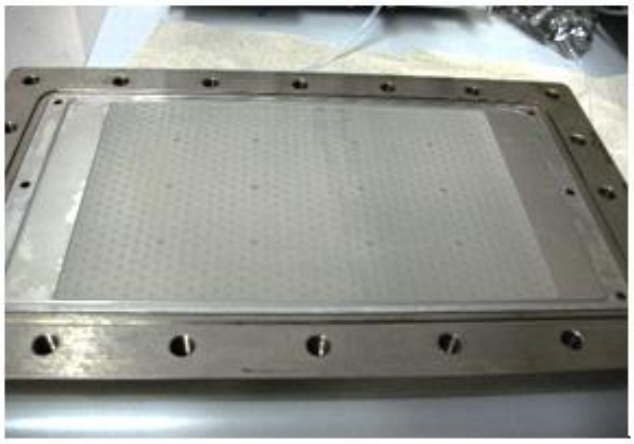

Figure 2. 7: The reactor bottom plate is shown loaded with an alginate layer with encapsulated cells.

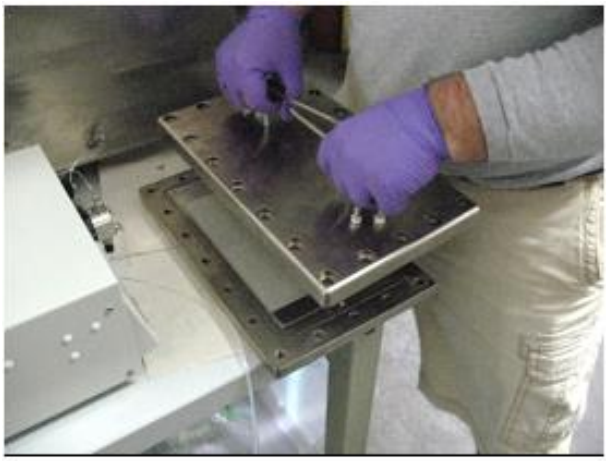

Figure 2. 8: Picture of the reactor clamp plates with attached reactor flow and base plates that are being assembled.

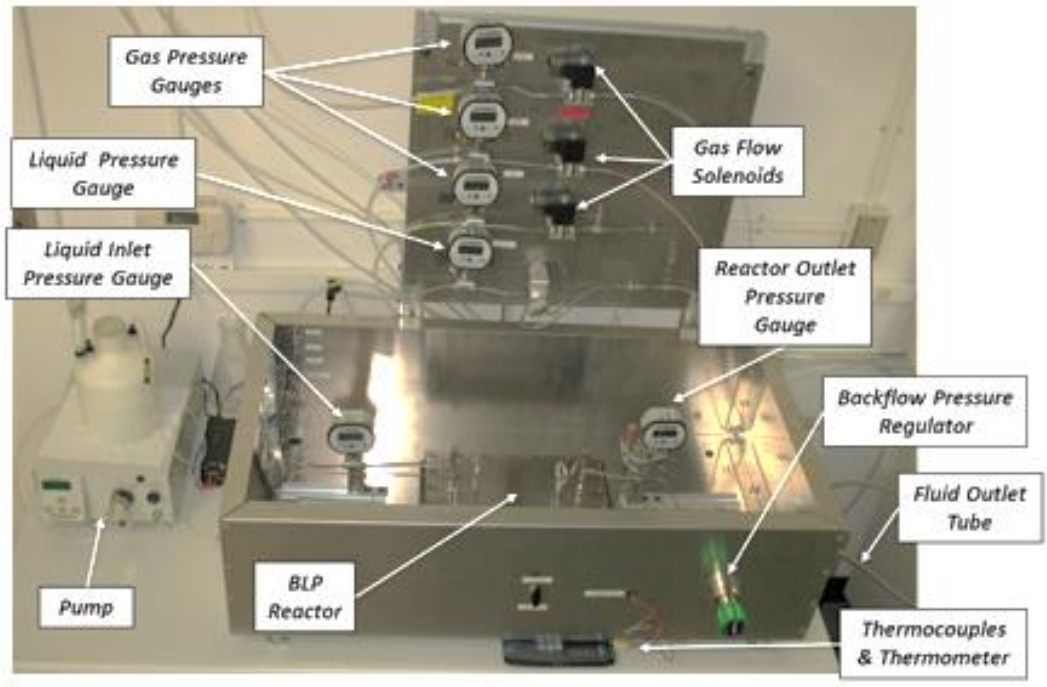

Figure 2. 9: The entire reactor system setup Locations of pressure gauges, gas flow controllers, HPLC pump, and other key parts of the system are labeled.

BLP Operation

A summary table of the BLP reactor experiments is shown in table D.1 in appendix D. For reactor startup, initially only liquid flow was introduced at a flow rate of no more than 2 mL/min for the first 10 minutes. After this, the flow rate could be increased slowly. After the liquid flow rate was set then gas flow was introduced into the system slowly. The pressure at the gas pressure gauges were set at twice the reactor pressure for steady state operation to insure proper flow distribution through the top reactor plate.

For all experiments, two phase flow was only introduced during the day when the reactor system could be monitored for problems. At night the gas flow was turned off until morning, but the liquid media was normally still introduced into the reactor. If the cells were being inhibited with cyclopropanol, then the cyclopropanol (made from alginate immobilized OB3b cells fed

with cyclopropane) was introduced into the reactor and allowed to remain in the reactor overnight. It was then flushed out with media the next morning and experiments would resume.

Inlet and outlet pressures and liquid flow rates were monitored and recorded throughout most experiments. Often, reactor experiments were halted due to excess pressure building up in the reactor. In later experiments, pH measurements of the outlet were taken as well.

After the reactor experiment was stopped then the reactor was disassembled and the integrity of the gel was analyzed qualitatively for both gel cohesion and adhesion properties.

Results

BLP Loading and Internal Gelation

Initial attempts at loading the base BLP plate with an alginate gel consisted of pouring liquid alginate into the plate and using a Teflon rod to scrape the alginate solution across the reactor. This would make the top of the liquid alginate flush with the top of the plate. The plate was then submerged in a calcium chloride solution to solidify the alginate through calcium crosslinking. When this procedure was implemented it was observed that the alginate gel pulled away from the wall of the reactor and did not produce a gel that was uniformly thick through the entire reactor (see figure 2.10). It was determined that this was caused by the calcium chloride solution washing the alginate out of the edges of the reactor before it could solidify.

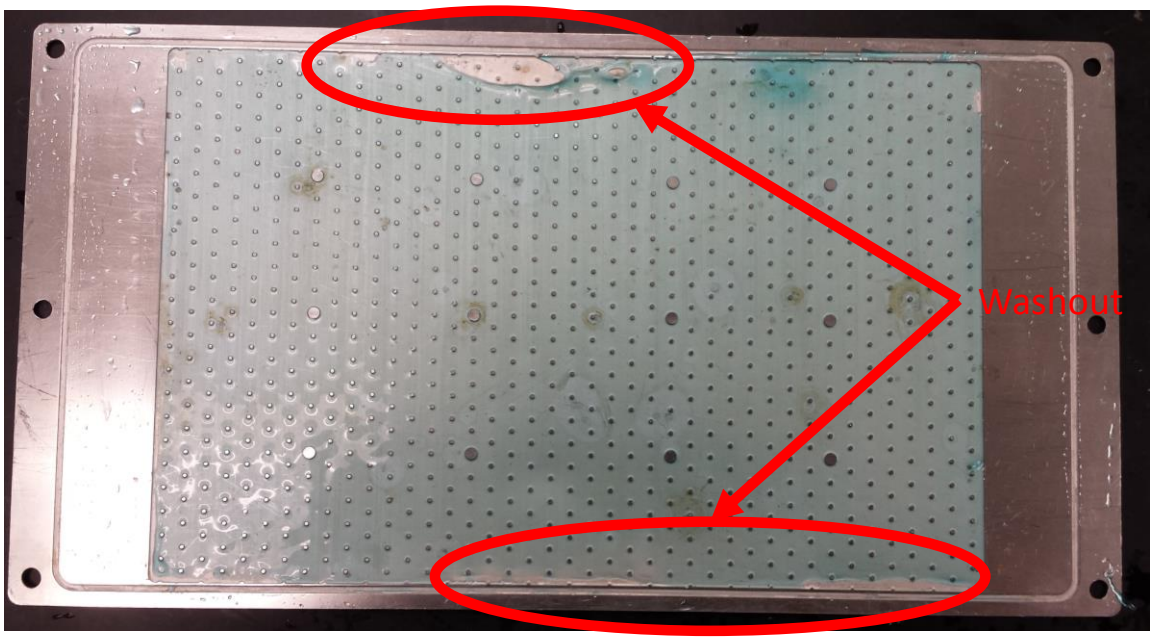

Figure 2. 10: Initial attempts at loading reactor base plates with alginate by submerging it with liquid alginate in $CaCl_2$ solution. The gel would separate from some of the sides of the reactor plate in this process and it was later determined that this was caused by liquid $CaCl_2$ solution washing out some of the alginate solution before it could solidify.

In order to remedy the washout problem, a spray bottle was used to mist the top of the alginate film with calcium chloride solution before a full submersion in calcium chloride. This caused the top of the alginate gel to solidify, giving the gel enough strength to resist the washout upon submersion. It was observed that if the misting is too slow and light then the surface of the alginate became rough and uneven and solidification will take place at some points before others. Misting should not be too harsh either, or else it would gouge out part of the film and cause deformities in the gel. The best method was to create a noticeable film of calcium chloride solution on top of the gel without disturbing the surface. This caused the alginate to solidify uniformly without making the surface rough.

Another method proved promising was based on work by Minjeong et al using internal gelation.[44] In this method, calcium is slowly released from calcium carbonate inside the gel by due to the addition of GDL. This calcium is then free to bind with the alginate causing it to

crosslink internally in the gel. By changing the concentrations of the calcium carbonate and GDL, the alginate solidification time can be controlled. Using this method, practically any shape that can be molded can be formed with the alginate (see figure 2.11). This is a significant advantage from external gelation because it does not rely on diffusion of calcium through the gel. This allows the gel to have a homogenous crosslinking structure throughout the entire gel as opposed to a tighter crosslink at the gel-calcium chloride solution interface.

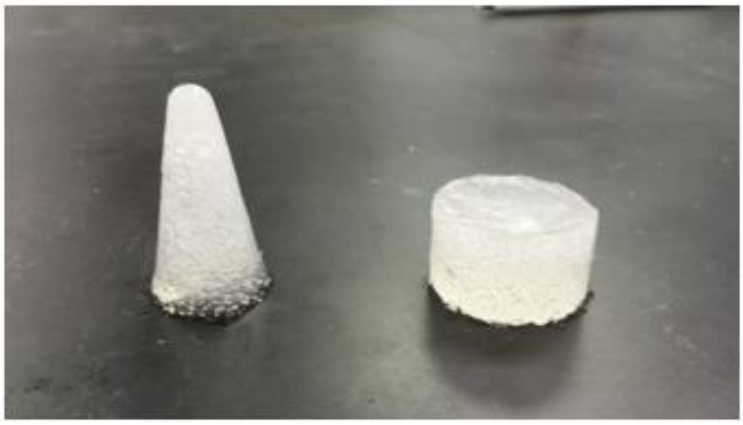

Figure 2. 11: Alginate gel shapes made with internal gelation. The internal gelation protocol allows for gels of any shape to be made. GDL and calcium carbonate were added to liquid alginate and over time the alginate would solidify homogenously throughout the gel.

For the purposes of using internal gelation in the BLP, it was desired for the gel to set within 10-15 minutes. This gave enough time to pour and level the gel in the bottom BLP plate. The gel could then be submerged in calcium chloride solution to give it some additional strength. It is worth noting that this process causes a lot of bubbles to form in the alginate solution due to CO_2 formation. These bubbles can get trapped in the gel matrix if it is solidified to quickly as seen in figure 2.11. For 500 µm films or less, a 5-15 minute gelation time was long enough for the bubbles to escape the alginate layer. However, for layers as small as 2 mm this is not adequate time for the bubbles to escape. If larger films or objects need to be made the concentrations of calcium carbonate and GDL need to be decreased to give the bubbles enough time to settle out of the gel before it solidifies.

Because of the ease of making gels with internal gelation and the homogeneity of the alginate film, it is the preferred method for making hydrogels in the BLP reactor. It has been used numerous times to produce uniform and stable hydrogels and it is more likely to produce a smooth gel layer than the spray method discussed.

Alginate Cohesion Studies in the Reactor

Initial experiments in the BLP reactor with an alginate gel in DI water showed no significant gel degradation nor swelling of the alginate hydrogel as seen in figure 2.12. This indicates that the shear effects of single phase liquid flow did not significantly affect the gel morphology.

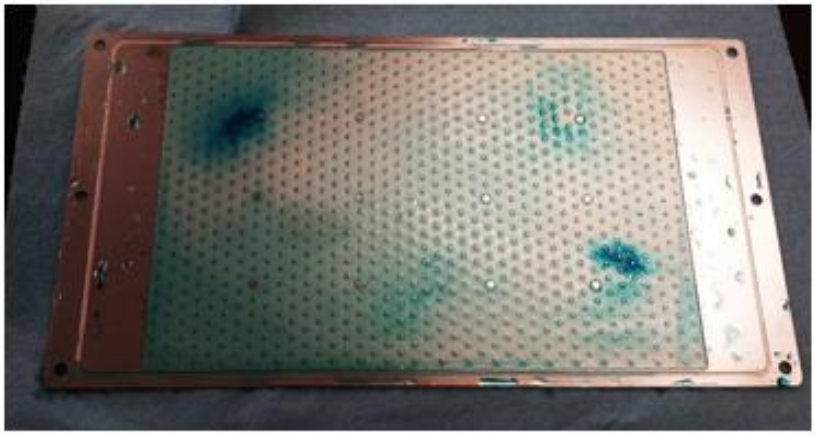

Figure 2. 12: The bottom plate with a gel in it after a reactor test with only DI water at a flow rate of 8 mL/min. The gel was dyed with food coloring at some spots to allow for easier visual inspection of the gel. The gel showed no degradation in this experiment.

Later reactor experiments with immobilized cells and two-phase flow showed significant gel swelling, gel deterioration, and flow channels being carved into the gel (see appendix D experiment 7 for conditions) as seen in figure 2.13. Initially it was thought that this may be due to the added shear effects of two phase flow on the gel. However, later experiments indicated that degradation occurred in single phase liquid flow as well. Furthermore, in future runs we were able to obtain stable alginate films with two phase flow as seen in figure 2.14 (see appendix D

experiment 11 for conditions). This indicates that shear effects from a two phase flow system were not the main cause of gel degradation.

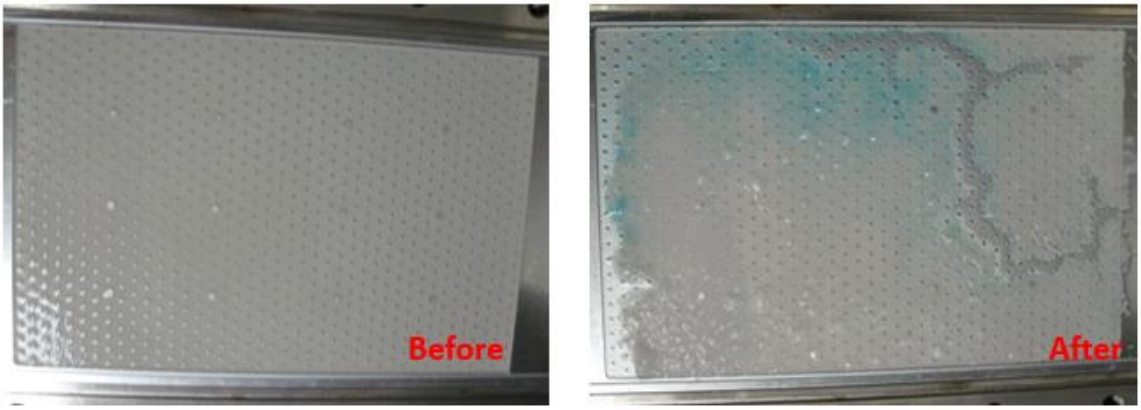

Figure 2. 13: Gels of a reactor plate loaded with OB3b before and after a reactor run. (a) A gel with OB3b cells before a reactor run is shown. (b) The gel in the same reactor plate after a reactor experiment (see appendix D experiment #7 for details) is shown. The gel was exposed to two-phase flow in phosphate media in this experiment. This media formulation had $1/10^{th}$ the desired amount of calcium chloride in it. The gel showed significant deterioration and the flow in the reactor made channels through the gel.

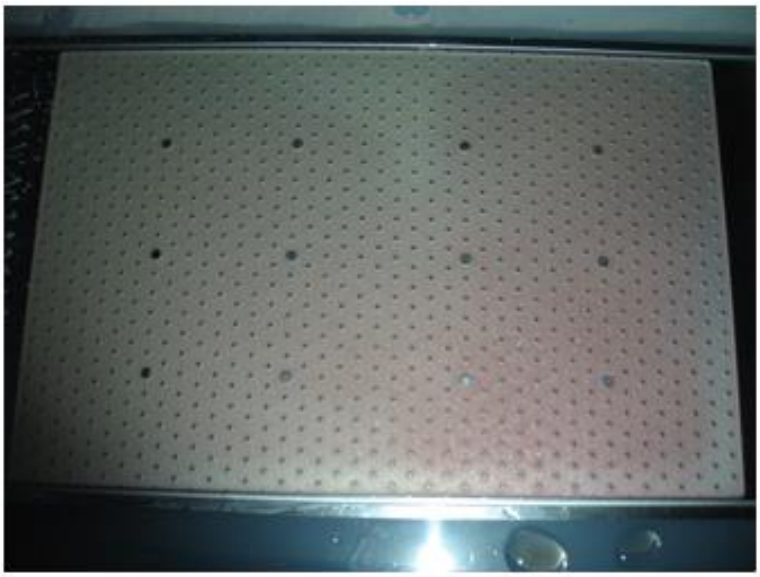

Figure 2. 14: A gel after reactor experiment # 11 (see appendix D for details). The gel was exposed to 2 phase flow in phosphate media in this experiment and had the proper amount of calcium chloride added.

Since shear effects did not seem to be the main cause of gel deterioration in the reactor, it was hypothesized that gel degradation was likely due to either effects of the media solution on the

gel or some effect from the metabolism of the cells. It is well known that alginate gels can be degraded over time in the presence of chelating agents.[32,33,34] Low pH conditions have also been shown to decrease alginate integrity.[35] The phosphate media that was used contained phosphate as a buffer and small amounts of Ethylenediaminetetraacetic acid (EDTA). Both of these are known calcium chelating agents which could have contributed to gel degradation. The cells also produce carbon dioxide in the final step of their metabolic pathway. Carbon dioxide can be dissolved into carbonic acid in water which can reduce the pH in the reactor, causing the gel to deteriorate (equation 2.1).

$$CO_2 + H_2O \rightleftharpoons H_2CO_3 \qquad \text{(Equation 2.1)}$$

Initial experiments in the BLP reactor were performed with 1/10th the amount of calcium that was supposed to be in the media formulation. This caused a substantial decrease in the amount of divalent ions in the solution, which could offset the effects of chelators and pH changes in the media. When the amount of calcium was corrected in the media (all experiments after experiment 9 in appendix D), the gel swelling was reduced and the integrity of the gel was greatly improved, though gels still noticeably weakened throughout reactor experiments. Unfortunately, while this change in formulation helped the gel cohesion, it also had detrimental effect on the reactor system as a whole. With the increased calcium concentration, a precipitate of calcium phosphate formed in the media solution. This precipitate to coated the orifices inside the reactor causing it to clog fluid and gas channels. This caused an increase in reactor pressure that eventually forced the end of the experiment.

To eliminate the problem of the calcium phosphate precipitate while still maintaining an adequate buffering capacity in the media, we tested the reactor with a HEPES buffer (experiment #14 in appendix D) as it does not have the chelation potential that phosphate does. This resulted in a very stable gel film at the end of the experiment (see figure 2.15) and the gel did not appear to swell. The solution also did not form a precipitate to clog the reactor in this experiment. It is

worth noting that the buffering capacity of the HEPES buffer was increased in this run, so it is still not clear from these experiments whether phosphate chelation of the calcium or a reduction in pH was the main cause of gel degradation in the earlier reactor experiments.

Figure 2. 15: A gel after a two-phase flow reactor experiment with HEPES media. The gel was noticeably stronger after this experiment than any experiment with phsophate media. The wrinkles in the gel are due to gel detachment from the plate.

Flow Cell Testing

In order to better understand the effects of solutions on the cohesion of the gel, microfluidic flow cells were constructed to mimic the operation of the reactor and can be seen in figure 2.16. These flow cells allowed for rapid testing of several media and solution compositions, as they are easier to assemble and operate than the BLP reactor. Also multiple flow cells can be used at one time. The flow cells were designed for single-phase liquid flow and had depth dimensions similar to the BLP. The flow cells were designed to have the same liquid velocity over the gel as in the initial BLP project proposal (most experiments thus far have been lower than this). This allows for the alginate to be exposed to the same amount of solution in both the flow cells and the BLP with the same shear forces. The flow cells were designed to test the

effects of solutions on the alginate through swelling and rheology tests that are described below. They also could be adapted for use in metabolic testing with dissolved gas species.

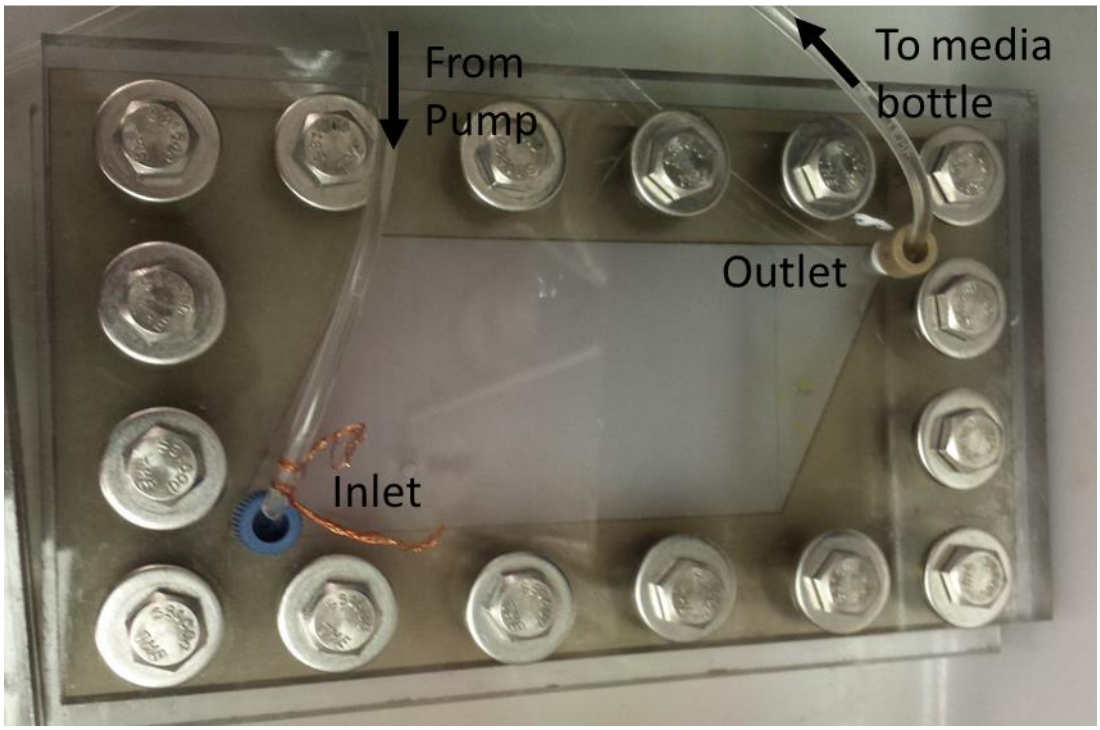

Figure 2. 16: A picture of a microfluidic flow cell. Media was perfused through the flow cell in order to examine the effects of various media compositions on the gel.

A little leaking was observed at the outlet ports of some of the flow cells. Putting Teflon tape around the threads of the outlet port helped mitigate some of this leakage, but not all of it. However a modest amount of leakage was deemed acceptable in these experiments and less than 5% of the total volume of the fluid basin was lost in each experiment.

Swell Test

Swelling of alginate hydrogels in media solutions is an important factor to control, as it can cause flow maldistributions in the reactor. After the flow cell tests were performed, the gels were inspected for significant swelling (see figure 2.17). Significant gel swelling was observed when the flow cells were exposed to acidic water and phosphate media. The gels exposed to acidic water showed swelling over the entire gel surface and was very rough. The gels exposed to

phosphate media tended to swell in larger blobs, resulting in smooth, large swollen bumps. The gels exposed to HEPES media showed mild swelling in small locations throughout the gel. It appeared to swell in a similar way to that of the phosphate media flow cells, but to a lesser degree. The gels that were only exposed to DI water showed no effects of swelling and looked similar to when they were originally loaded into the flow cells.

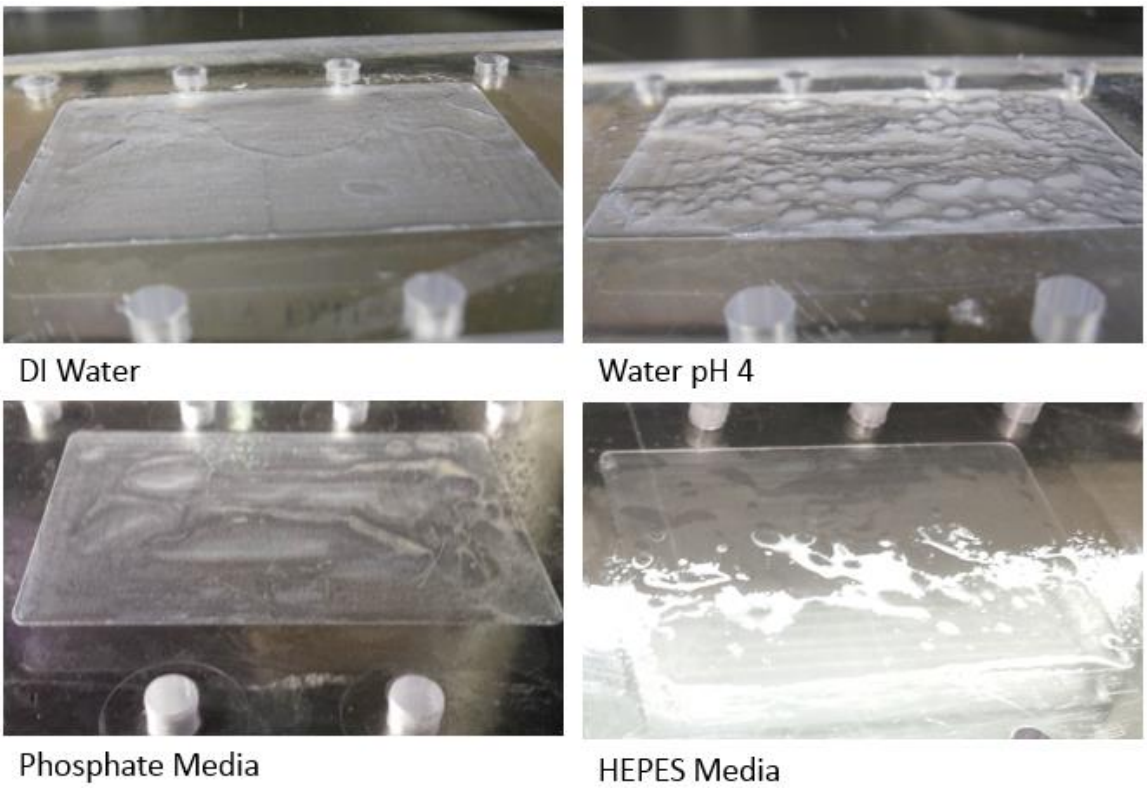

Figure 2. 17: Pictures of gel swelling after flow cell perfusion with various media and solution compositions. Acidic water and phosphate media caused significant swelling and surface roughing. HEPES media caused mild swelling and the DI water caused no noticeable swelling.

In order to quantify the amount of swelling that occurred in the flow cells, swell depth was measured using a microscope and a micromanipulator with step control to probe the gel depth with a needle. The depth of the gel above the sidewall of the well was measured at the highest and lowest points of the gel along with a point that was representative of the median gel height. Two gels that were exposed to each media composition were analyzed (figure 2.18).

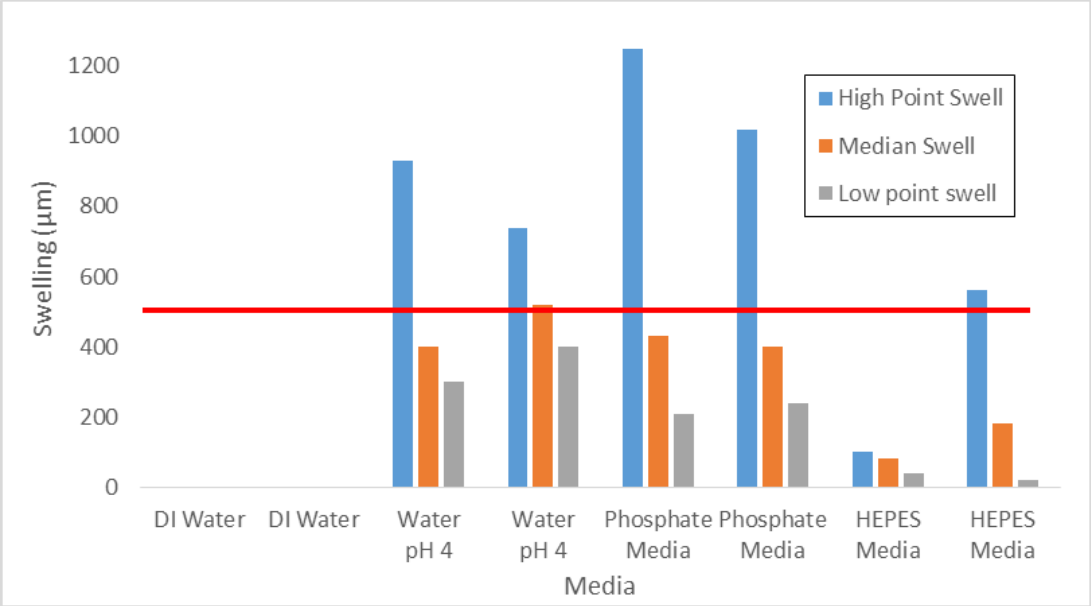

Figure 2. 18: Swell test data from flow cell experiments. The height of the alginate gel at its highest and lowest point along with a median swell point is shown for two flow cells operated under various media conditions. The red line represents the height of the flow area in the flow cell, so gels at that height would have fully occluded flow. The results show significant gel swelling in acidic water and with phosphate media. Modest swelling was observed with the HEPES media, while no swelling was observed with perfusion of DI water.

The phosphate media and the acidic water showed the most swelling. In both, there were points at which the gel had fully occluded the flow of the microfluidic cell. In all of the flow cells exposed to these media, the median swelling of the gel was at least 400 µm. This means that in much of the flow cell, the flow path was less than 100 µm, indicating a significant change in the flow distribution through the cell.

The gels exposed to the HEPES media showed mild swelling of the alginate films. While in one of the flow cells there was a one or two points in which the gel swelled up to the top of the flow cell, the number of points that swelled to this height was minimal, indicating that not much of the flow area was completely blocked. The median swelling point in one of the flow cells was 180 µm and 80 µm in the other. This shows flow blockage of 16-36%. While this is a notable amount of blockage, it is significantly better than the effects of the phosphate media.

The flow cells exposed only to DI water showed no evidence of swelling whatsoever. This indicates that flow of liquid over the gel does not promote gel swelling in and of itself. Therefore it must be components of the media introduced into the gels that promote the swelling.

From these tests it is apparent that highly acidic environments are very detrimental to the gels. Since the final product of OB3b metabolism is CO_2 which can make water acidic, it is very important to buffer the BLP in order to avoid acidification of the gel. In some of the first BLP experiments in which pH was measured, the pH of the outlet media was observed to be 5.8 (Appendix D experiment 10). This is a marked increase in the acidity of the media and it is likely that the local pH of the gel in some areas was even lower. It is worth noting that the gel in that experiment was significantly degraded after the experiment.

Based on a comparison of the HEPES and phosphate media results, it is apparent that phosphate is detrimental to gel integrity. The only difference in the media compositions was the substitution of HEPES for phosphate as a buffer. These results seem to indicate that the phosphate in the media can leach calcium from the gels over time which causes them to swell and degrade.

The HEPES caused some mild gel swelling and degradation by itself. While the amount of swelling observed was much less than that of the acidic water or the phosphate media, it is still a enough swelling that it could interfere with operation of the BLP. No mechanism is known for HEPES to directly leach calcium from alginate. This fact coupled with the significant improvement of HEPES media solution over phosphate solutions would indicate that it is likely other components of the media that cause the gel to degrade. The most likely cause for this degradation is that the monovalent cations in the media are competitively displacing the calcium in the alginate. Since sodium and potassium are needed for biological function, there is no way to completely remove these monovalent cations from the system. In order to prevent degradation of the gel in HEPES media, other options must be devised in order to offset the effect of these cations.

Rheology

In an attempt to quantify the effects of various media compositions on alginate hydrogels in the flow cells rheological studies were performed. In these studies, the flow with attached gel was mounted to the bottom of a rheometer and oscillatory rheometry was performed. Rheological studies were performed on the flow cell experiments with DI water flow and with acidic water. The results from the rheological studies can be seen in figure 2.19.

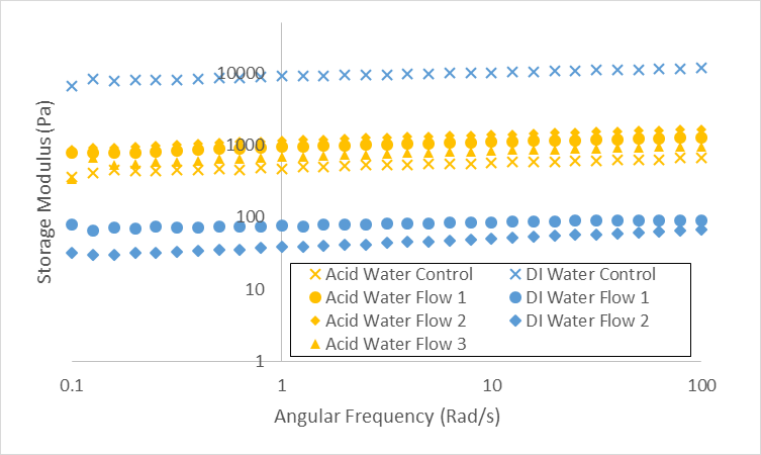

Figure 2. 19: Rheological data from flow cell tests. DI water and acidic water were perfused through the flow cells. Oscillatory rheology was then performed on the alginate samples from the flow cells.

The results from the rheological studies show that the alginate exhibits typical gel behavior with a storage modulus that responds linearly with angular frequency (on a log scale). The controls for both sample groups were made from the same gel solution as the flow tests and were stored in DI water while the flow tests were being run. The results show that there was a loss of storage modulus when the gels were exposed to flow with DI water. This indicates that there may be a reduction in cohesive properties of the gel from shear flow alone. While this data indicates that the gel may degrade under DI flow, the swell tests have shown that there is no

swelling due to DI water flow, so it is unknown whether the shear stress of flow weakens the gel to point that it could affect reactor performance.

The rheological studies for the acidic water flow cells show that the storage modulus increases compared to the control that was stored in DI water. This would normally indicate that the gel is more cohesive under the flow of acidic conditions. However this is directly contradictory to gel morphology and swell studies. Currently it is thought that the reason the acidic water storage modulus is calculated to a higher value in these tests is that the depth of the gel is not constant between samples. Gel depth is a factor in the calculations of the shear modulus, and because the gel swelled significantly throughout these experiments it is no longer constant. This skews the calculations of the bulk modulus and makes the comparison between the gels impossible.

Another problem with rheometry related to the gel swelling is that the gel swelling is not uniform. Full contact with the top of the gel by the steel rheometer plate is necessary for accurate measurements. Since the gel swelled more in some areas than others, the full gel does not contact the plate properly making the measurements inaccurate.

Another potential problem for rheology with the flow cells is that the distance from the bottom of the flow cell plate to the base of the well may not be perfectly constant between the flow cells. We are reasonably confident that the depth of the flow cells are very close to 500 μm from the top surface, but the thickness of the polycarbonate may be somewhat variable. The specifications from the McMaster-Carr website where the polycarbonate was purchased indicates that tolerances should be within 0.019” which is about 480 μm. Since the gel films are 500 μm these tolerances could provide a huge source of error between gel samples. One possibility to reduce this error could be to increase the depth of the gel. Another possibility would be to detach the gel from the surface of the flow cell and put it directly on the bottom rheometer plate. This

latter idea could be difficult to implement for significantly weakened gels as the adhesion of the gel to the surface may make it difficult to pull the gel out of the flow cell in one continuous film.

It is currently unknown how to mitigate the problems with using rheology with samples from the flow cells. It might be possible to cut the gels to a specific thickness if they swell, but this will likely prove logistically difficult and hard to control. It is also unknown whether the inhomogeneity of gel degradation may skew rheological results unpredictably. More work on method development of rheology is required to obtain accurate results in our systems.

Limitations of flow cells

Because the logistics of creating a two-phase flow device was deemed impractical for the time frame provided in this project, the flow cells were designed for single-phase flow only. This established several limitations on the use of the flow cells. Firstly, the shear forces that the alginate is exposed to in these flow cells are not the same as two phase-flow. While shear forces do not seem to be the main cause of cohesive failure in the BLP system, they may contribute to the problem in a minor way. Secondly, because the flow cells were not designed for two-phase flow, the addition of bubbles may cause more leaking in the system, causing a potential safety hazard as the gas mixture is flammable. Furthermore, the addition of gas bubbles in the flow cells may be difficult to distribute evenly throughout the flow cell. It may be possible to establish slug flow in the reactor by injecting bubbles into the feed line, but this would not mimic the distribution and size of bubbles in the BLP. Lastly, the flow cells are made out of polycarbonate and not stainless steel. While the direct attachment of the alginate to the surface of the flow cell and the reactor APTMS coatings, the attachment of the APTMS coating itself to the surface is very different. This means that the flow cells are not well suited to the testing of effects of various solutions and shear flow on the adhesion properties of the gel to the surface.

Conclusions and Future Work

Early experiments in the BLP reactor showed noticeable gel deterioration in the reactor. Initial problems of gel integrity in the BLP were mitigated by increasing the concentration of calcium in the reactor. However, this caused calcium deposit buildup on the orifices of the reactor resulting in a pressure increase in the reactor. HEPES media was then used, which prevented the calcium buildup and produced stable gel films throughout the experiment. This is likely due to both the prevention of calcium chelation from the alginate due to the phosphate, and an increased buffering capacity of the HEPES media. These changes caused the gel to remain stable for the entirety of a BLP experiment.

To diagnose the direct cause of gel degradation in the BLP system, microfluidic flow cells were made that mimic some of the flow conditions in the reactor. Various liquid conditions were perfused through the flow cells to see the effect on the gel. Phosphate and acidic conditions significantly degraded the gel and caused it to swell. Flow cells that had DI water perfused through them appeared unchanged indicating liquid flow itself did not affect the gel integrity enough to affect flow distribution. The flow cells that were perfused with HEPES media showed slight swelling and degradation of the gel, but much than with the phosphate media and acidic water tests. This degradation was likely due to the monovalent salts in the media which are necessary components of the media and cannot be eliminated. Because of the increased buffering capacity and the lower degradation of the gel with the HEPES media, it is the preferred media solution going forward with the BLP.

Rheology tests were attempted on some of the flow cell gels. Rheology proved to be ineffective for measuring alginate cohesion due to the fact that gel swelling affects the depth of the alginate gel, which alters the results obtained by the rheometer. Furthermore, inconsistencies

in the exact depth of the flow cells also can skew the results. Further work in developing methods is needed before they become useful to test gel integrity.

More work is needed to diagnose the causes of gel degradation in the BLP and to determine the best encapsulation method and media formulations. The flow cells can be used to rapidly test a variety of media formulations and flow conditions. In the future, these flow cells should be loaded with alginate-encapsulated OB3b to determine the effects of media formulations on gel with living cells.

Other immobilization media should also be tested. There are currently plans to attempt to immobilize OB3b on nanosprings which would eliminate the swelling problem currently encountered in our system. Other immobilization mediums, such as agar, could be used that do not leech ions over time and degrade. The effects on cell viability from the heating and cooling of agar immobilized cells would have to verified as well in these tests.

Tests should also be performed on the method of alginate crosslinking. It is well known that other divalent ions such as Sr^{2+} and even some trivalent ions can be used to crosslink alginate gels. These cross-linking ions may be more resistant to leaching from chelators and monovalent ion displacement. Long-chain positively charged molecules such as polylysine should also be tried as crosslinkers, as they may be less apt to be displaced from the gels. Covalent crosslinking of alginate hydrogels should also be tested.

Furthermore, techniques should be developed to better quantify gel degradation in these systems. It may be possible to develop rheological techniques to test these gels if further work is done on method development in order to solve the problems listed above. Compression testing should also be looked into, as it may not have the same limitations based on alginate thickness that the rheology tests do.

Chapter 3

Alginate Adhesion

Introduction

Strong adhesion of alginate hydrogels to the reactor surface is important for the BLP reactor system. In order to keep the cells immobilized in the reactor, the alginate must be adequately anchored to a surface. If the alginate is not adequately anchored it might detach from the surface causing disruption of the fluidics in the reactor system and potentially clogging the reactor.

The reactor design of the BLP seems to be unique for the immobilization of cells. Most bioreactors with alginate immobilized cells consist of packed beds with cells encapsulated in gel beads. In these systems, gel beads just need to be prevented from exiting the reactor systems and could be easily immobilized in the reactor using a mesh filter at the outlet. In the BLP design, the gel must remain attached to the bottom surface, making the immobilization of the gel layer by adhesion an important part of the reactor system.

Little research has been found on the adhesion of alginate hydrogels onto flat surfaces such as the BLP reactor. There is a little research that has come out recently that where alginate gels have been conjugated with 3,4-dihydroxyphenylalanin to improve the adhesion strength to biological scaffolds which was inspired by mussel adhesion to surfaces.[37,38] In these studies, improved alginate adhesion to biological and glass surfaces was obtained.

While there are some studies discussing the alteration of alginate to improve adhesion to surfaces, another approach is to modify the surface to promote adhesion. Cleaning and oxidation of surfaces by UV-ozone has been shown to make surfaces more hydrophilic.[39] This can increase interactive forces between hydrophilic polymers and the surface, thus increasing the adhesion strength as well. Conjugating aminosilanes to a surface can also improve adhesion for negatively

charged polymer gels such as alginate (see figure 3.1 for reaction scheme). The amine terminal groups on these coatings when protonated have a positive charge which allows for electrostatic attraction of the negatively charged carboxyl groups on the alginate.

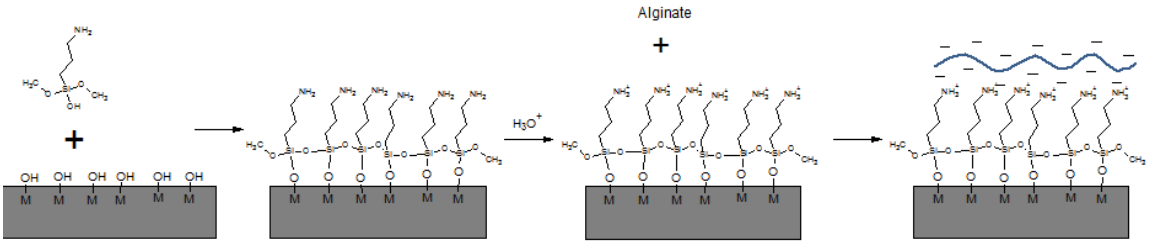

Figure 3. 1: Reaction scheme for APTMS coating of metal surfaces. APTMS can form siloxane bonds with hydroxyl groups of a metal surface. The polymer can then crosslink with other silanes on adjacently bound APTMS molecules creating a dense layer of amine terminated silanes on the surface. These amines can then be protonated with acid which gives them a positive charge that allows for electrostatic attraction with alginate.

In this chapter, alginate adhesion to treated steel surfaces is investigated. Various different surface treatments such as UV/ozone passivation, APTMS treatments, and polylysine coatings were investigated. Adhesion of alginate gels in the reactor system is discussed. Furthermore, adhesion tests using an Instron mechanical tester were performed to quantify alginate adhesion to steel. An investigation into adhesion on APTMS treated polycarbonate is also investigated.

Materials and Methods

Aminosilane functionalization of Stainless Steel Gel BLP Plate

Stainless steel BLP bottom plates were silanized with 3-aminopropyl trimethoxysilane (APTMS) (Sigma Aldrich CAS: 13822-56-5) in order to improve gel adhesion to the stainless steel surface. BLP plates were cleaned on a shake plate (60 rpm) by submersion in: acetone, RO water, toluene, acetone, and again in RO water. For the organic solvents the plates were washed for 15 minutes in each, and for the RO water the plates were washed for 5 minutes. After the BLP

plates were thoroughly cleaned, the reactor plate was passivated with 32.5% nitric acid for 30 minutes.

After passivation, the reactor plates were submerged in a 246:3:1 solution of 200 proof ethanol, water, and APTMS for 1-2 hours to allow the APTMS to react with the stainless steel. The reactor plates were then heated to 125 °C in an oven for 2 hours to cure. Any excess APTMS solution was then washed off the plate by submerging it in 140 proof ethanol twice for 10 minutes. This procedure was originally based off the procedure developed by Chuang et al,[40] and was modified to prevent vertical polymerization of the APTMS.

After initial use of the BLP bottom plate, or upon storage for more than 24 hours, the plate would be washed with ethanol for 10 minutes on a shake plate (60 rpm). It would then be submerged in 1% citric acid for 15 minutes in order to reprotonate the amine bonds on the APTMS. The plate would then be rinsed with RO water and air dried before use.

BLP Reactor Testing

See reactor section of Chapter 2 (Alginate Cohesion) for methods dealing with reactor operation.

Silanization of Stainless Steel Shims

Stainless steel shims were silanized with APTMS in order test gel adhesion to stainless steel surfaces and to treat any surfaces that were used in other tests (such as drip flow reactors). Stainless steel shims were made by cutting 0.024” thick 316 L stainless steel (McMaster-Carr #88885K81) into 1” x 3” pieces. The shims were coated in the same way as the silanization of the BLP plate, except that passivation was done using a UV/ozone cleaner for 10 minutes per side.

Polycarbonate Shim Silanization

Polycarbonate shims were treated with APTMS prior to adhesion strength testing. 1/16” thick polycarbonate pieces (McMaster-Carr #1749K72) were cut into 1” x 3” shims. The pieces were washed by submersion in ethanol for 10 minutes. The shims then were then coated with

APTMS solution (same recipe as above) and cured in the same manner as the stainless steel shims. The shims were then rinsed in ethanol twice for 10 minutes. On some shims, a second layer of APTMS was applied in the same way as the first coating.

Polylysine Coating of Stainless Steel

Metal shims were coated in polylysine in order to improve gel adhesion to stainless steel surfaces. Shims were cleaned and passivated as done in the stainless steel shim APTMS treatment. Immediately after passivation, the shims were coated in a polylysine solution (0.1% w/v H_2O) (Sigma-Aldrich #: P8920) for 8 hours, then washed off with water.

Alginate Adhesion Testing

Stainless steel shims underwent either solvent cleaning only, UV-ozone passivation, aminosilane treatment, or coating with polylysine prior to testing. Polycarbonate shims underwent either just ethanol cleaning, one APTMS treatment, or two APTMS treatments prior to testing. A 500 µm film of alginate was coated between two treated stainless steel or polycarbonate shims covering an area of 1" square of the shim surface by using internal gelation protocol. While still liquid, alginate with GDL and $CaCO_3$ added was poured onto a treated shim. A 500 µm thick stainless steel spacer was placed on the shim and a glass microscope slide and a glass slide was placed adjacent to the end of the slide. Another treated shim was placed on top of the glass slide and spacer to make a film that adheres to both shims (see figure 3.2). The alginate was left to set for 15 minutes and then the shims were submerged in a 0.1M $CaCl_2$ solution overnight for further crosslinking.

Figure 3. 2: A schematic of the setup to attach alginate to shims for strength testing. A 500 µm layer of alginate is formed between two treated stainless steel. Internal gelation is used to solidify the alginate.

Once the alginate was fully crosslinked, the glass slide and steel spacer were removed. An Instron mechanical tester (model # 5763) (see figure3.3) was used to obtain data on the strength of the alginate adhesion to the shims. About 1 inch of the end of one of the stainless steel shims was placed in the bottom clamp of the Instron. The top clamp was then adjusted to make sure it was properly positioned as to prevent a torque from being applied to the alginate when the clamp was shut. The top clamp was then shut and the shim setup was submerged underwater. The Instron was set to measure stress as the steel shims were pulled away from each other at a rate of 1.33 mm/min (based off of ASTM Standard D-1002-10).[41] After several minutes of being pulled apart the stress on the system would sharply decline indicating the breaking stress at which the alginate peeled from the surface of the steel. The breaking shear could then be determined by dividing the breaking stress by the covered surface area of the slides. After each test, the shims visually inspected to determine whether the system failed due to cohesive or adhesive failures of the alginate. At least 5 replicates were done for each surface treatment.

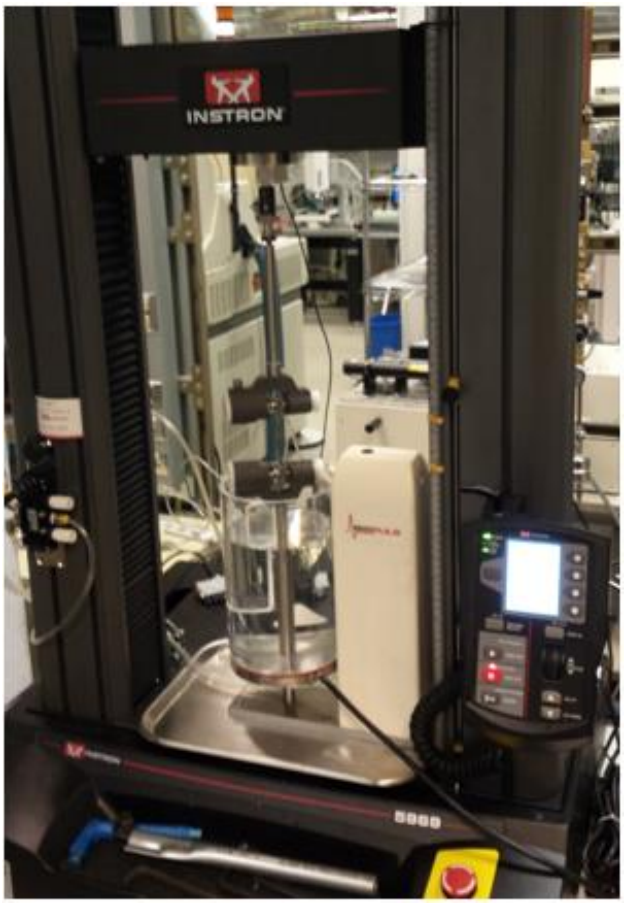

Figure 3. 3: A picture of the Instron mechanical tester. Two shims with a layer of alginate between them were clamped into the machine and then pulled apart in order to determine the shear force at which the alginate will break from the shim surface.

Results and Discussion

BLP Reactor

Initially it was estimated that the posts in the base plate of the reactor may be sufficient to anchor the alginate to the bottom reactor plate during reactor operation. Tests were done on both stainless steel shims and in a reactor plate to see if alginate adequately adhered to the stainless steel base plate. It was observed that without solvent cleaning, the alginate was repelled from the steel surface. This is likely due to oils and other contaminants being deposited on the reactor plate either from stainless steel processing or from the environment, which are hydrophobic and can

repel the alginate. While solvent cleaning helped the situation, the alginate did not adhere to the steel surface and tended to ball up on the reactor bottom plate.

To try to further improve alginate adhesion, stainless steel surfaces were passivated using a UV/ozone cleaner. This helped to noticeably increase the alginate's attraction to the steel surface and the alginate would better wet the surface. The surface wetting and improved adhesion is due to the oxidation of the steel surface, which allows the alginate and water to hydrogen bond with the surface oxides. This was a noticeable improvement over cleaning the steel alone, but the alginate still did not stick to the surface as desired. Because the UV/ozone cleaner that was used was too small to contain a reactor plate, reactor plates were passivated with nitric acid, which had a similar effect.

Because of the shear forces in the reactor, it was determined that passivation alone was not likely an effective surface treatment as it was likely that the gel would slough off the surface. To improve the adhesion of alginate to the steel, the steel was treated with APTMS. This treatment covalently bound a positively charged amine layer on the surface of the reactor. After this treatment, the alginate was electrostatically attracted to the surface and formed a stable adherence.

The reactor plate was then tested in the reactor system. After 2 hours of flow, no detachment of the gel was observed on the APTMS-treated reactor plate (see figure 3.4). This treatment was used on all successive reactor plates, and the gel appears to remain attached to the plate during operation in most of the BLP reactor experiments. However, the gel often detached from the surface in the reactor disassembly, due to a suction force applied to the gel during reactor disassembly. Because of this, it is hard to determine definitively whether or not the gel is detaching from the surface during the experiment; however, in most instances, it appears that the gel detaches in a way consistent with a suction force being applied, as one side of the detached with the other remaining intact. In the latest reactor experiment using HEPES, it appears that the

gel may have detached from the surface during the experiment as seen in figure 3.5 (see appendix D experiment 14 for conditions). This is evidenced by the way the gel detached over the entire reactor plate and by how the pressure increased in the reactor over the course of the experiment. It is likely that this detachment is either due to inadequate cleaning of the reactor plate or due to a degradation of the APTMS coating after several months of use. Some studies have shown that hydrolytic cleavage of the siloxane bond at surface can be catalyzed by the intermolecular amine group.[42] This indicates that over time the APTMS coating will start to degrade.

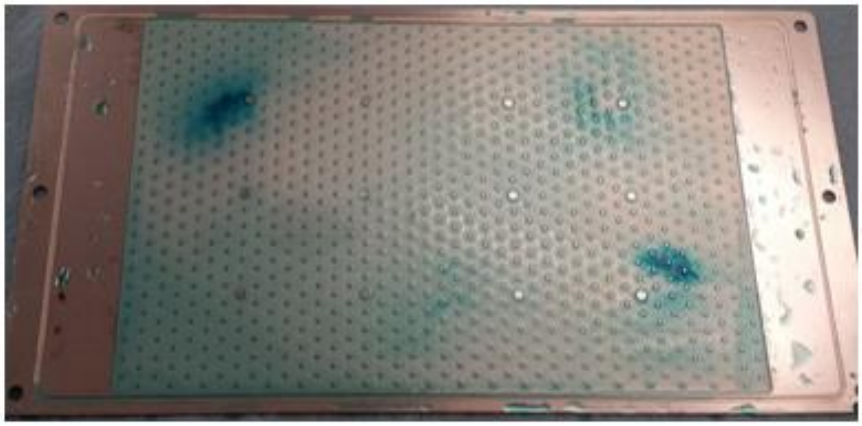

Figure 3. 4: The bottom plate with a gel in it after a reactor test with only DI water at a flow rate of 8 mL/min. The gel was dyed with food coloring to allow for easier visual inspection of the gel. The gel adhered well to the surface of the reactor and did not pull away at any part.

Figure 3. 5: A gel after a two phase flow reactor experiment with HEPES media. The gel seems to have detached from the surface during the reactor run. It is likely that this was due to the degradation of the plate APTMS treatment, but effects of the new media solution cannot be ruled out.

Before the latest experiment, it was observed that when making a gel film on this plate that the alginate tended to recede from spots on the plate, indicating that they may have become hydrophobic. Adhesion in those areas would be minimal in the reactor system and would contribute to adhesion failure. While it is most likely that the cause of detachment was a degraded or dirty coating, effects of the HEPES media on the system cannot be ruled out at this time.

Adhesion strength to Steel

In order to better compare the adhesion strength of alginate to various surfaces, adhesion strength testing was performed on an Instron mechanical tester. Stainless steel surfaces were coated with polylysine, conjugated with APTMS, or cleaned with no further treatment. An example of the data obtained from the Instron machine can be seen in figure 3.6. A summary of the data from this experiment can be seen in figure 3.7. The data shows that both the APTMS and polylysine treatments provide significantly enhanced adhesion strength compared to the untreated

steel. The polylysine sample shows slightly better adherence strength than the APTMS sample, but this difference is not statistically significant.

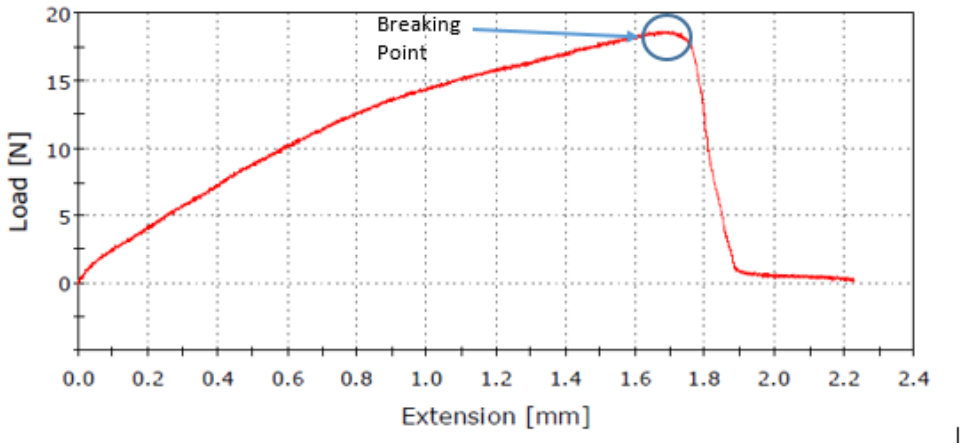

Figure 3. 6: An example of the raw data from adhesion tests with the Instron machine. The stress (load) is measured as the shims are pulled away from each other. At the breaking point the stress drops suddenly and the breaking shear can be determined.

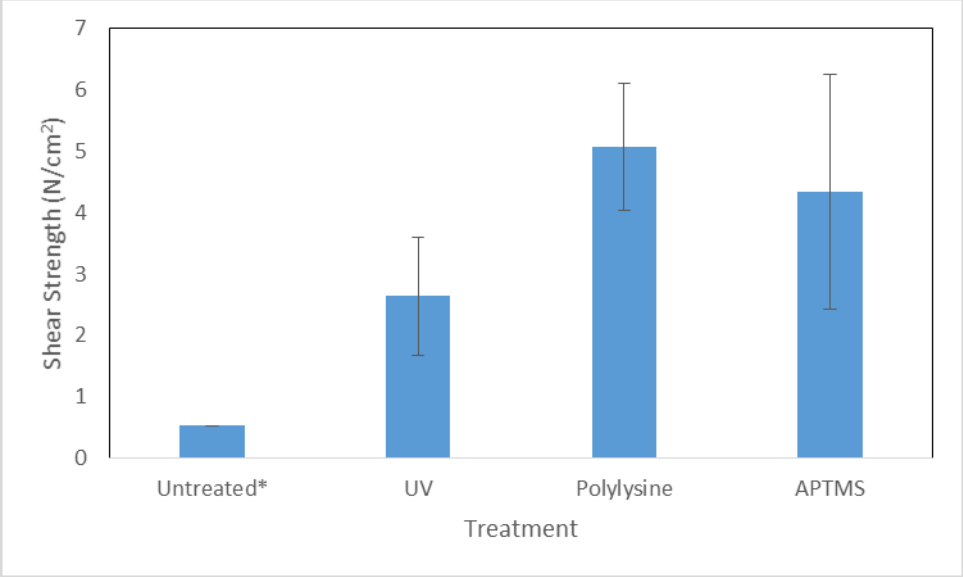

Figure 3. 7: A summary of data obtained from the Inston tests on stainless steel. Both the APTMS and polylysine surfaces show significant adhesion improvement over UV ozone treatments and untreated steel. UV ozone treatment showed some improvement over untreated steel. Error bars based on a 95% confidence interval. *Only one data point for untreated steel was obtained, because most samples fell apart as they were being loaded on the instron.

In all instances, the alginate broke away from the surface of the steel indicating that the adhesion force of the gel to the surface was overcome before cohesion failure in the gel. Sometimes the alginate broke only from one surface, indicating that the gel adhered better to one of the slides, and sometime part of it broke from one and part of it from another, indicating that the adhesion strength on both slides was similar. Pictures of what the gels look like after the adhesion test is shown in figure 3.8.

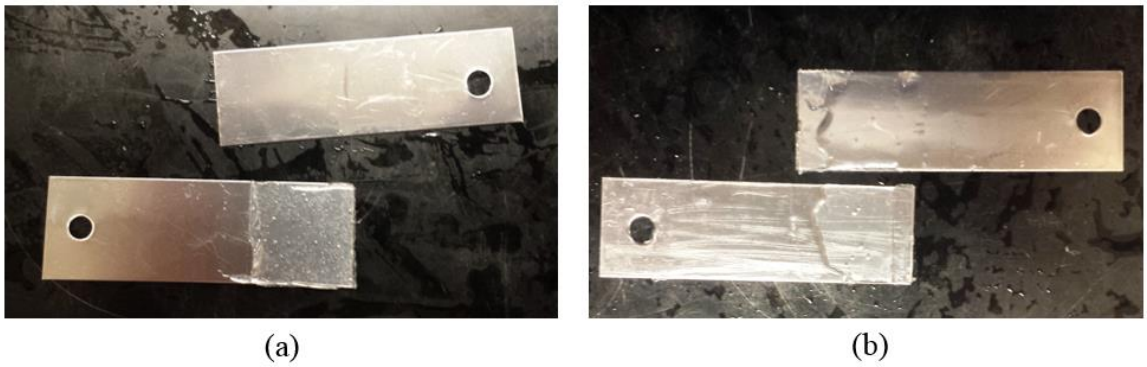

Figure 3. 8: Example pictures of APTMS treated stainless steel slides after adhesion testing. In (a) the gel delaminated from one surface only while in (b) the gel delaminated partially from both surfaces. In both instances, the gel detached from the surface indicating the gel cohesion forces are stronger than the gel adhesion force to the steel.

It was very important when performing these experiments that the shims be straight and perfectly aligned. Early attempts at strength testing used steel that was slightly bent producing inconsistent results. It was also observed that if the slides were not perfectly aligned on the Instron machine that the breaking strain tended to be lower, presumably due a torque being applied to the steel surface that pulled on the alginate. At times it was difficult to align the shims properly as the pneumatic clamps on the machine closed very quickly with substantial force. This often caused the shims to misalign which applied a torque to the gel prior to testing.

Adhesion strength to Polycarbonate

A future goal of this project is to be able to manufacture the BLP reactor out of plastic to reduce the capital cost of the system. To this end it is necessary to be able to attach the alginate gel to a plastic surface. Polycarbonate was identified as an ideal choice because it has good

mechanical strength and optical transparency which, makes it easy to characterize the flow conditions inside the reactor.

Alginate adheres to untreated polycarbonate worse than it does to untreated stainless steel. While alginate does not adhere well to stainless steel surfaces, it is not actively repelled by them either. Polycarbonate surfaces repel alginate and alginate will often float off of a polycarbonate surface that it is put on. For this reason, polycarbonate must be chemically modified with something to which the alginate can adhere. Since APTMS coatings worked well on stainless steel, it was tried on polycarbonate as well.

On stainless steel, the silane of the APTMS attaches to the hydroxyl groups on the steel surface. This orients the terminal amines in the APTMS up towards the alginate gel (see figure 3.1). Current research on the coating of polymers with carboxyl groups, such as polycarbonate, with aminosilanes, results in the amine group pointed down towards the polymer surface.[43,44] It is hypothesized that a urethane linkage between the polymer and amine side of the aminosilane can then form.[44] In the case of APTMS, this would leave the silane groups oriented away from the plastic. Practically this leaves a layer of glass on the surface from which other compounds can be bound. It is proposed that if another layer of APTMS is added, then the silane groups on the new APTMS and the surface coating will occur with amine groups now pointed upwards. A schematic of this proposed reaction scheme with APTMS can be seen in figure 3.9.

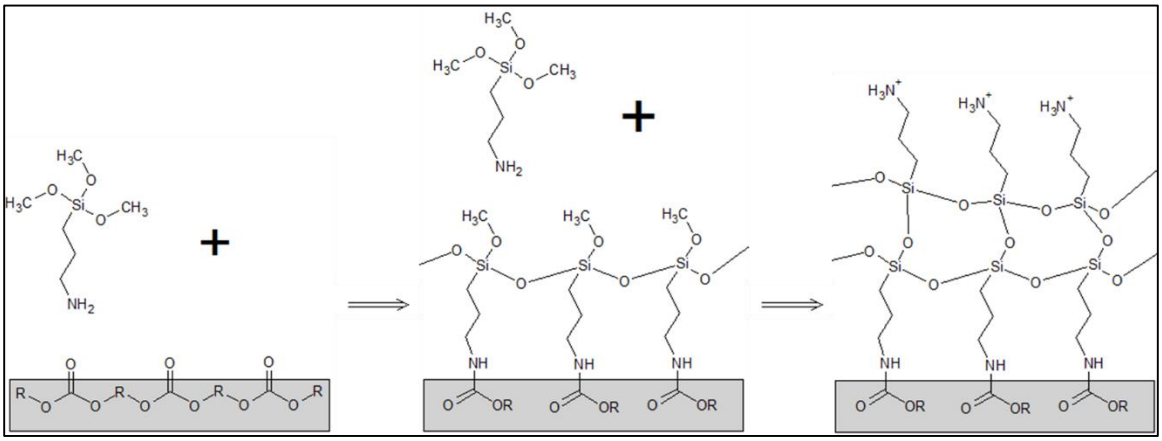

Figure 3. 9: A proposed mechanism for double APTMS coatings of polycarbonate, based on a mechanism from Jang et al.[44] The amine groups of the APTMS are conjugated to the polycarbonate through urethane bonds in the first APTMS coating. A second APTMS coating is then applied forming siloxane bonds with the first APTMS coating resulting in amines being oriented away from the PC surface.

To test this hypothesis polycarbonate shims were coated once in APTMS. A subset of these shims were then coated again with APTMS. These shims were then tested for alginate adhesion using the adhesion strength protocol described earlier.

The results from the strength testing of APTMS coated polycarbonate can be seen in figure 3.10. Both PC with one APTMS coat and PC with two APTMS coats showed improvement over uncoated PC, which did not adhere to alginate at all. The twice APTMS coated PC showed much higher adhesion than the single APTMS coated PC and had a similar adhesion strength to APTMS coated steel. These results indicate that a second APTMS coating increases the adhesion strength of alginate to polycarbonate.

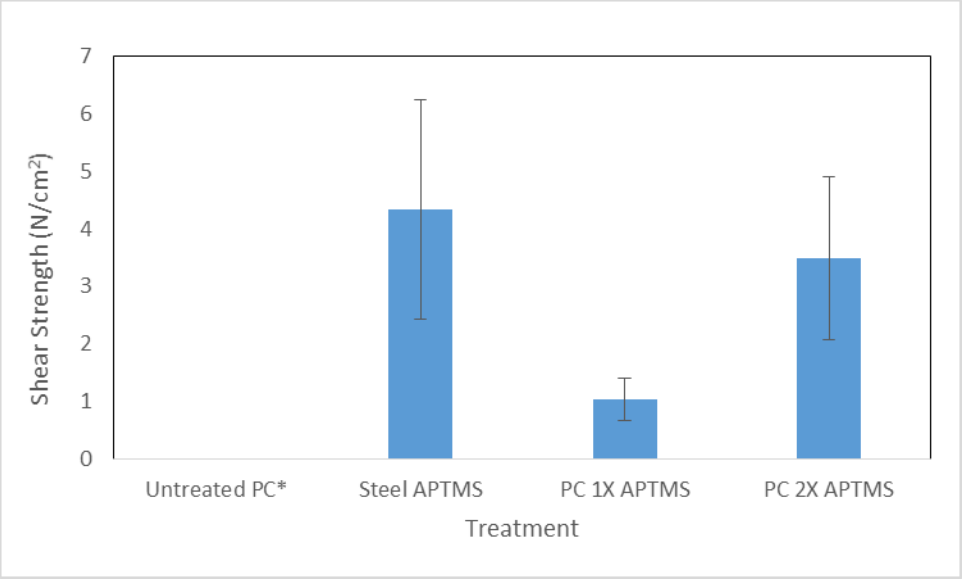

Figure 3. 10: A summary of data obtained from the Inston tests on polycarbonate. APTMS on steel is shown as a comparison. PC treated with APTMS twice had similar adhesion as the APTMS treated stainless steel. The PC with only one APTMS coating showed some improved adhesion over untreated PC, but not as much as on the twice treated PC. Error bars are based on a 95% confidence interval. * Untreated samples could not be tested on the machine, because untreated polycarbonate repelled the alginate.

The increase in adhesion strength from the second APTMS coating could be due to one of two factors. If the hypothetical reaction scheme found in figure 3.9 is accurate, then the increase in adhesion strength is likely due to the orientation of the amines. Another possibility is that the second APTMS coating simply created a denser surface layer of aminosilanes. This would allow for more interaction with the APTMS coating and less interaction with the polycarbonate, which would increase the adhesion strength. Further surface analysis of the APTMS layer on the PC is necessary to prove one scenario over the other.

There has been some concern in studies that APTMS attachment to PC may be prone to hydrolysis.[44] It is unknown whether this hydrolysis is faster on polycarbonate than on other surfaces. A proposed solution to prevent hydrolysis is to use bis[3-(trimethoxysilyl)propyl]amine (bis-TPA) for the surface attachment to PC.[44] The reaction with secondary amines is thought to be more resistant to hydrolysis than primary amines like APTMS.

Conclusions and Future Work

While alginate has comparable adhesion strength to both polylysine and APTMS treated stainless steel, APTMS is the preferred treatment. It is believed that the polylysine treatment adheres to the stainless steel surface only through electrostatic adhesion. While this adhesion is strong, there is concern about how stable the treatment will be after extended use. On the other hand, the APTMS treatment covalently binds the APTMS to the steel surface and has been shown to be effective after multiple reactor experiments. Hydrolytic cleavage of the siloxane bonds may cause the coating to degrade over time and would require that the reactor plate coatings be reapplied from time to time, however APTMS coatings have proven to be stable through several reactor experiments. Another reason APTMS is preferred is cost. The APTMS treatment is considerably cheaper than the polylysine treatment, as it costs less than $2 per reactor plate treatment as compared to ~$20 per treatment for polylysine.

Surface functionalization of PC was also investigated in order to examine the possibility of making the BLP out of polymers, which would considerably lower the price of the system. APTMS treatment of the surface was shown to significantly increase adhesion strength of the alginate to PC. A second coating of APTMS proved to be beneficial for added adhesion strength. This is likely due to the alignment the amines on the APTMS towards the alginate, but the increased adhesion strength could also be due to a denser coating of amines on the surface.

The viability of these APTMS coatings on PC are further validated by their ability to anchor the alginate in the flow cells discussed in chapter 2. In all of the flow cells, the alginate was shown to adhere to the surface without detachment during flow. Furthermore no mechanical structures (such as posts) were required for increased adhesion in these flow cells like there are in the BLP. These factors make APTMS coatings on polycarbonate surfaces an effective method for surface functionalization moving forward with plastic BLPs.

Further studies on surface adhesion of alginate gels and other mediums remains to be done. A study of how long it takes APTMS both stainless steel and on PC to be hydrolytically cleaved from the surface should be done. Furthermore, it is worth testing secondary aminosilanes such as bis-TPA on polycarbonate, to see if it forms a more stable coating. Surface analysis could also be done on APTMS-conjugated polycarbonate to determine whether the amine group orientation is the factor that makes PC coated with APTMS twice a better surface for alginate adhesion than single coated APTMS PC. It would also be interesting to perform strength testing on glass slides to see if the adhesion strength is similar to single APTMS coated PC. This may indicate that the first APTMS coating simply puts a layer of "glass" on the surface, from which further coatings can be attached.

It may be desirable in the future to use immobilization media other than alginate. The strength testing procedure developed here should work with a variety of different media. It may be further valuable to test these medium under flow using similar flow cells to those described in chapter 2. New flow cells could be machined out of PC with a deeper alginate well. Various substrates with different surface coatings could then be inserted into the well of the PC to test the adhesion of the immobilization medium under flow. This would allow for rapid testing of surfaces without the need to put them in the BLP, which is very time consuming.

Chapter 4

Cell Viability and Reactor Performance

Introduction

One of the most important aspects for successful cell immobilization is keeping the cells viable throughout the encapsulation process. Cells that do not survive the encapsulation process are useless in the system. Therefore, it is imperative that the encapsulation process take place under mild conditions, to maximize cell survival.

While there are many different potential encapsulation media for our system, alginate was chosen because it can be gelled under relatively mild conditions. Alginate hydrogels have been used for cell encapsulation in a number of applications.[22,27,28] In all these applications, a majority of the encapsulated cells survived alginate immobilization after the process was optimized.

There are several factors that could potentially kill the cells in the encapsulation process. In other encapsulation media, cells may be exposed to potentially inhospitable conditions. For example, agar can be used for cell encapsulation by heating and then cooling it. While this encapsulation method may be effective in some circumstances, the cells must be able to withstand the thermal shock of being heated. Polyvinyl alcohol (PVA) has also been used as an immobilization medium using boric acid as a crosslinking agent.[45] For some types of cells, the boric acid could prove toxic causing PVA to fail as an encapsulation medium.

Some potential hazards to OB3b encapsulation in alginate were considered in our system. One problem with our immobilization process is that we must remove the OB3b from its metabolic substrate (methane) during the encapsulation process. Long term removal from a suitable substrate could cause the cells to die from starvation or enter a dormant state. Another potential problem with alginate encapsulation is that calcium chloride is a known inhibitor of both

MDH and MMO. The addition of calcium chloride to the system could inhibit cellular metabolism causing them to turn over methane slowly.

Surviving the encapsulation process is only half the issue for cell viability the BLP reactor. The cells must also survive during reactor operation. One factor affecting cell performance and viability in the reactor system is the diffusion of substrate through the alginate in the reactor. The immobilization media must not trap the substrate or significantly inhibit its diffusion to the cells. Alginate has been shown to allow diffusion of uncharge molecules of up to 150 kDa without significant diffusion inhibition.[28] Methane and oxygen are four orders of magnitude smaller than this and there is no physical reason to believe that their diffusion would be seriously inhibited through the gel. Another potential problem that may affect cell viability in the film, is that the substrate could be completely consumed in the top layers of the film. This would leave the bottom layers of the film starved for substrate. For this reason, the depth of the alginate layer and concentration of cells in the alginate should be optimized.

Process conditions could also kill the cells in the BLP. If not properly encapsulated shear forces could potentially kill or strip away the cells in the top layers of the alginate. Pressure fluctuations in the reactor could also damage the cells to lyse if they occur too quickly. Temperature conditions in the reactor should also be monitored to ensure that it remains within acceptable physiological levels.

In this chapter, cell viability in the alginate hydrogels is investigated. Live/dead staining of cells was performed to determine if cell lysis occurred during the gel encapsulation process. Their ability to metabolize in batch systems was also investigated. At the end of this chapter, preliminary BLP performance data is discussed and compared to the free cell performance found in a chemostat system.

Materials and Methods

Live/Dead Staining

Live/Dead staining was performed using a Life Technology BacLight™ Live/Dead staining kit (L13152). The kit contains Syto 9 as a live cell stain and propidium iodide as a dead cell stain. Cells were obtained from the chemostat that Tanner Bushnell maintained. Cells were washed and resuspended in phosphate buffer (PBS) in a live control and in 70% ethanol for a dead control. Cells were incubated for 1 hour in these solutions and were then resuspended in PBS as a control or in liquid alginate (final alginate concentration 2 wt%). The alginate samples were then crosslinked using either the external gelation protocol or the internal gelation protocol. Dye solutions were made following instructions in the BacLight™ manual. The dye solutions were added to the solution controls at a 1:5 ratio giving a final Syto 9 concentration of 2 μM and a final propidium iodide concentration of 10 μM. These solutions were then incubated for 15 minutes. For the alginate gel samples, the gels were covered in 20 μL of each solution (twice as much as in the solution samples) and incubated for 20 minutes. The samples were then imaged under a fluorescence microscope using a GFP filter for the live stain, a Texas Red filter for the dead stain, or a long pass filter to see both stains simultaneously. Pictures of the live and dead stains were taken with a mounted camera and cells were counted using Image J (NIH).

Metabolic Function in Batch Tests

OB3b cells were encapsulated in alginate beads at a concentration of 1 g/L. Gel beads were formed by extruding cell-loaded liquid alginate solution from a 23 gauge needle into a 0.1M calcium chloride bath. 10 mL of beads and 8 mL of phosphate growth media were put into sealed vials with 9 mL of head space. For free cell tests, an equivalent amount of cell mass was added to a vial with a combined cell and media volume of 18 mL, leaving the same amount of head space

as the immobilized cell experiment. The vials were left for 200 minutes and the methane in the head space was analyzed using a Shimadzu Chromatopac C-R8A gas chromatograph.

BLP Reactor Performance Tests

See reactor section of Chapter 2 (Alginate Cohesion) for methods dealing with reactor setup and operation. See Appendix D for reactor conditions and results.

For the methane consumption tests, media saturated with air and methane were fed into the reactor system. Inlet and outlet samples were taken from the reactor at various time points. These samples were analyzed for methane concentrations using gas chromatography and the methane consumption was calculated from the difference.

For methanol production tests, methane and oxygen bubbles were perfused through the reactor, keeping the levels of these gases at saturation conditions in the media. OB3b cells were inhibited by the addition of cyclopropanol overnight, unless otherwise stated in Appendix D. Media samples were taken at the outlet at various time points. The methanol concentrations of the samples were analyzed by gas chromatography, and methanol production rates were calculated from these concentrations.

Chemostat Tests

The chemostat was maintained by Tanner Bushnell and activity tests were performed by him as well.

A 7 L chemostat was filled with 3L of phosphate media (see Appendix C for recipe). The chemostat was inoculated with OB3b cells and grown to a concentration of about 0.3 g cell protein / L. The media flow rate in the chemostat was 0.6 L/day, making the retention time in the reactor 5 days. Methane was fed into the reactor at a rate of 0.14 mmol/hr and air was fed to the reactor at a rate of 1.56 mmol/hr. The impeller speed in the chemostat was set at 300 rpm.

Methane consumption was quantified by sampling the vapor phase effluent of the chemostat. 1 L of chemostat effluent gas was obtained and 10 mL of propane was added to the

effluent gas as an internal standard. The effluent gas was then analyzed by GC-FID. Calculations of methane consumption were then based off of the inlet and outlet methane flow rates and the composition of the effluent gas.

Inhibition of the cells in the chemostat was achieved by pulsing cyclopropanol into the system. Final concentrations of cyclopropanol in these pulses ranged from between 0.05mg/L and 2.4 mg/L. In inhibited tests methanol concentrations in the outlet were determined by analyzing the effluent aqueous phase by GC. The flow rate and methanol concentration of the reactor effluent were then used to determine methanol production rates.

Results and Discussion

Live/Dead Staining

Live/Dead staining was performed to determine whether the OB3b cells survived the alginate gelation process. Controls of the stains in the solution show that the stains work generally as expected (see appendix B). When the cells were dead in solution they only fluoresced with the Texas Red filter; when they were alive they fluoresced with the GFP filter. Under the long pass filter the live cells fluoresced green and the dead cells fluoresced yellow or red. All these cells were easily distinguishable as live or dead.

The stains did not work in exactly the same in the gel as they did in solution. When cells were live they fluoresced only green as expected, but when the cells were dead they fluoresced red and green under the Texas Red and GFP filters respectively as shown in figure 4.1 (a) and (b). Under the longpass filter, the cells fluoresced yellow, making them hard to distinguish from the live green cells (see figure 4.1 (c)) This made the longpass filter ineffective for use analyzing cells within a gel layer.

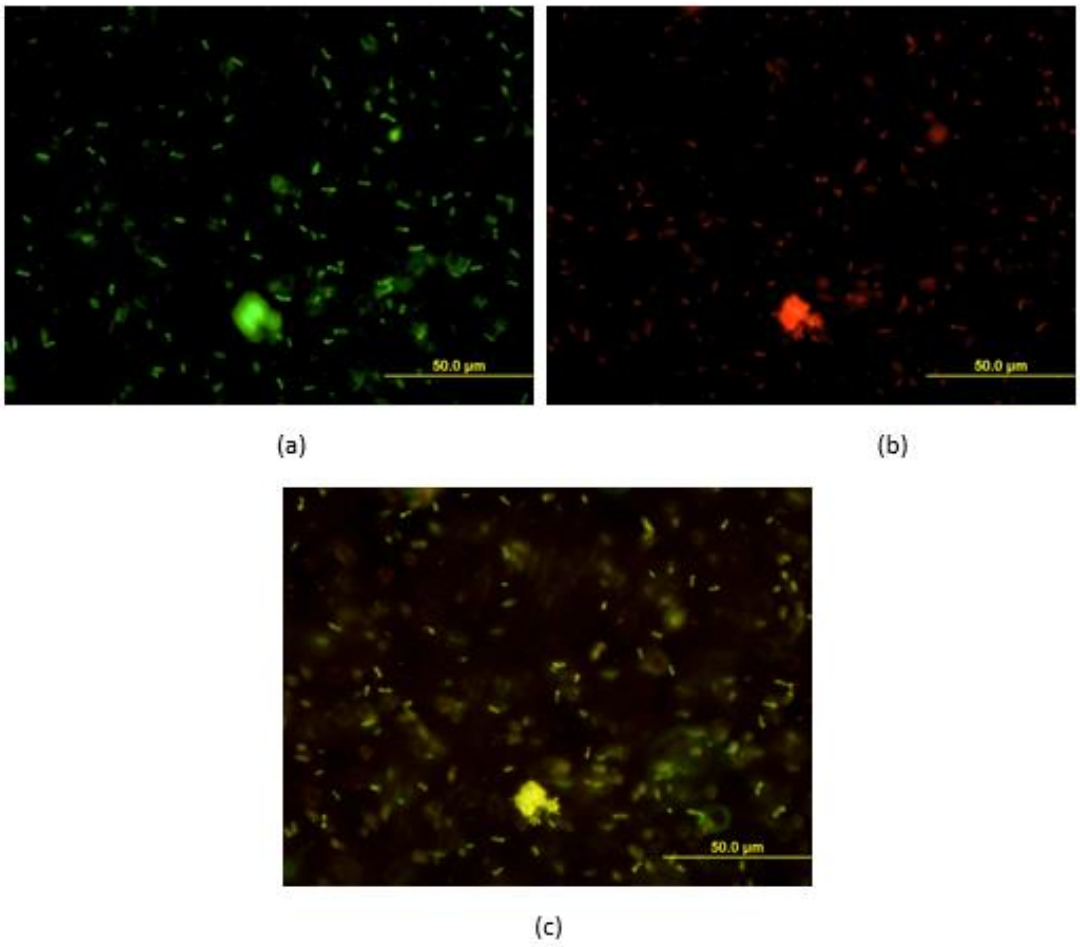

Figure 4. 1: Images of OB3b cells in an alginate hydrogel after they were lysed with 70% ethanol. (a) shows cells through a GFP (live) filter, (b) shows cells through a Texas Red (dead) filter, and (c) shows cells through a longpass filter (simultaneous live and dead). Dead cells in an alginate gel were shown to fluoresce both red and green with these solutions.

Because all cells fluoresced green in the gel and only the dead cells fluoresced red, the number of live cells in a gel layer could be determined by simply subtracting these quantities. An analysis of this technique was performed on the dead cells in alginate shown in figure 4.1 and a 4% difference was observed in the quantities of cells that fluoresced green and red. This difference was deemed acceptable for these studies.

The live dead staining shows that over 93% of the cells survive the external gelation process with external gelation in calcium chloride as seen in figure 4.2. Furthermore under the

internal gelation process, there was no significant cell death detected (see figure 4.3) though the cell densities in this study were significantly lower than in the external gelation study. This data indicates that OB3b cells are likely still viable through the alginate encapsulation process using both methods.

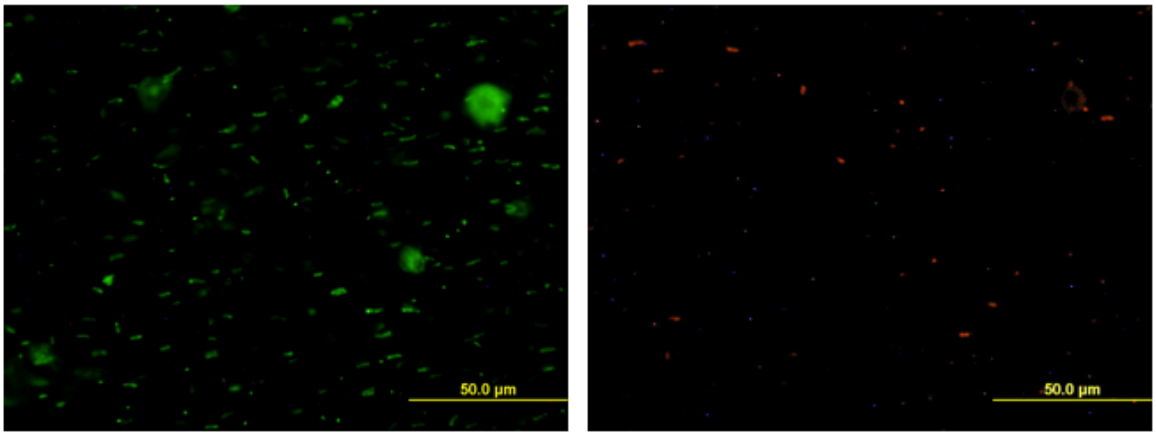

Figure 4. 2: Live/Dead images of OB3b cells in an externally crosslinked alginate hydrogel. (a) shows cells through a GFP (all cells) filter and (b) shows cells through a Texas Red (dead) filter. Analysis of these images showed that 93% of cells survived the gelation process.

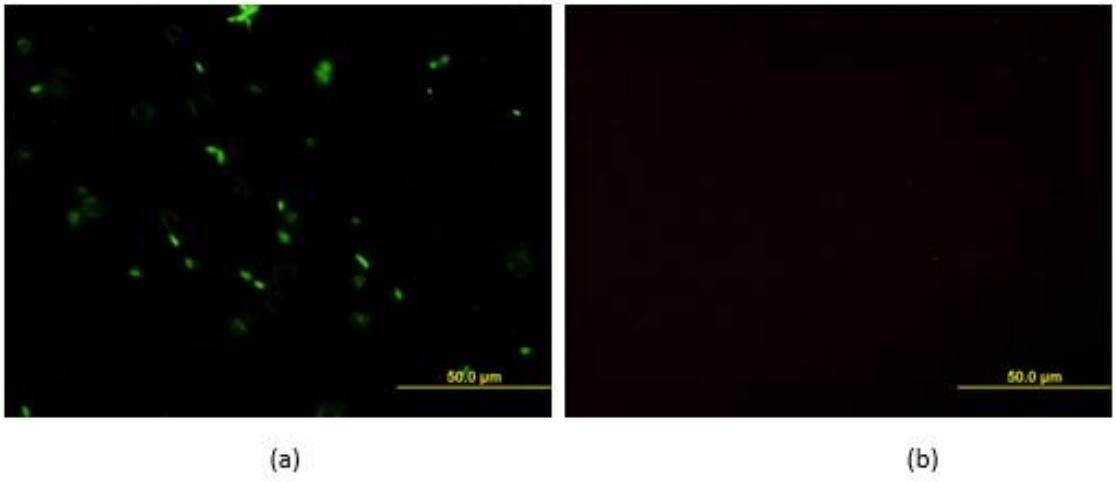

Figure 4. 3: Live/Dead images of OB3b in an internally crosslinked alginate hydrogel. (a) shows cells through a GFP filter (all cells) and (b) shows cells through a Texas Red (dead) filter. Analysis of these images showed that all cells survived the gelation process.

It is worth noting that these live/dead staining only determines whether or not the cells have an intact membrane. It will not determine if the cells are metabolically inactive or died due

to some mechanism internal to the cell. Coupled with metabolic tests, however, it can be a great asset in analyzing cells in alginate suspensions.

It is difficult to use the live/dead staining to analyze the cells from a reactor experiment using our current scope. Figure 4.4 shows images of an OB3b loaded hydrogel after a reactor experiment. The cell density in these studies are too high to see individual cells under the microscope that was used. A general green and red haze is seen instead which makes analysis of the gel with this scope ineffective. It may be possible however to use a confocal fluorescence microscope to look at these gels. A confocal microscope could image a single plane through the gel and filter out much of the interference from cells above and below the focal plane. This would make quantifying cells in the gel much easier and cells at higher densities could be quantified. A depth profile of the cells could also be done which would allow for the determination of whether some cells are being starved or poisoned in the reactor system.

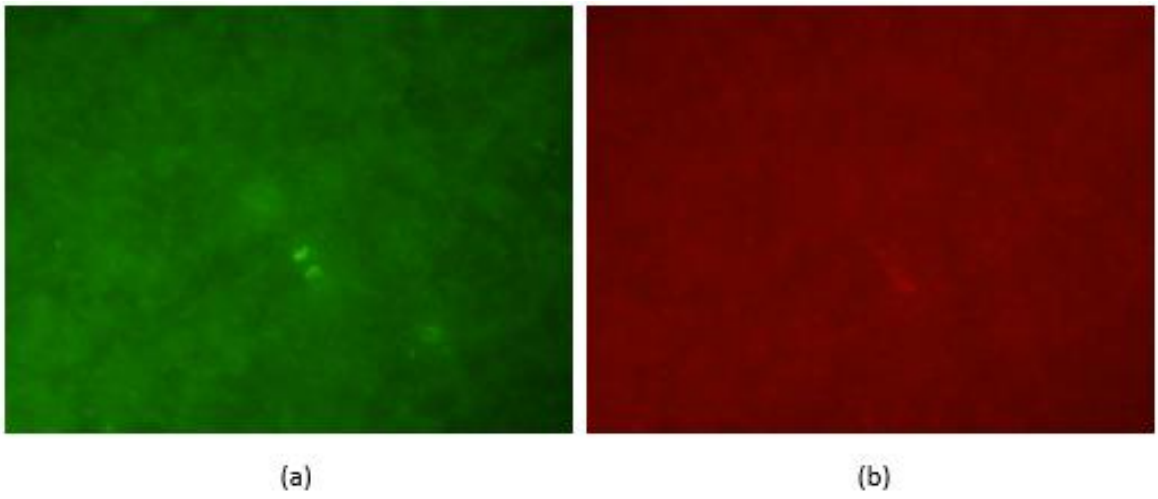

Figure 4. 4: Live/Dead images of OB3b after a reactor experiment are shown. (a) shows cells through a GFP (live) filter and (b) shows cells through a Texas Red (dead) filter. The cell densities in the reactor were too high to be able to quantify the cells.

Metabolic Function in Batch Tests

A summary of a comparison between batch metabolic studies with immobilized cells and free cell suspensions is shown in figure 4.5. Cells were immobilized in gel beads that were on

average 2.5 mm in diameter. The cells in the free suspension converted 93% of the methane after 200 minutes and the immobilized cells converted 77% of the methane in the same amount of time. This indicates that the immobilized cells retained about 83% of their activity when immobilized in alginate beads. While it is probable that some of the reduction in OB3b activity was due to the immobilization of the cells themselves, some of the reduction can also be attributed to diffusive resistance in the alginate beads. It is expected that an alginate layer of about 300 µm in the BLP to have appreciably less diffusion resistance than a 2.5 mm bead. Overall, these tests prove that OB3b encapsulation in alginate does not kill or halt cell metabolism. However they do not give much information on methane consumption rates of OB3b in alginate.

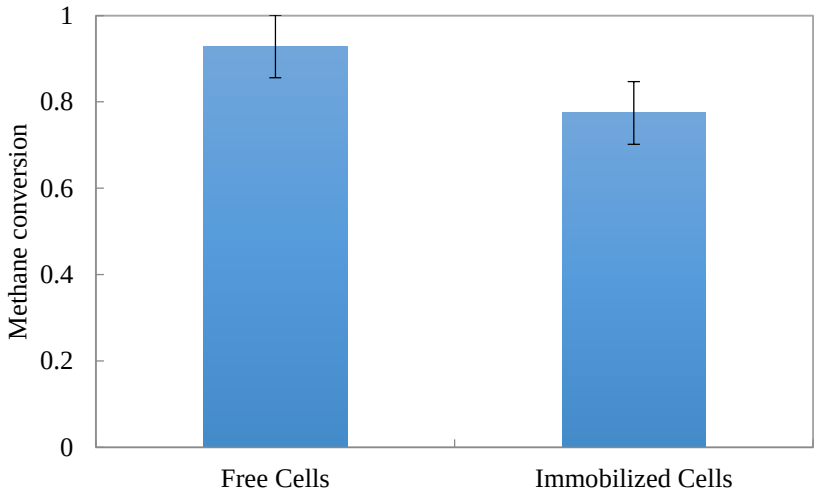

Figure 4. 5: A summary of the data from batch methane conversion studies with alginate bead encapsulated cells and free cell suspensions. Solutions were exposed to a methane header for 200 minutes and the methane in the head space was measured. The free cells consumed 93% of the methane and the immobilized cells consumed 77%, so the immobilized cells showed a decrease in activity of 83%.

Immobilized Cell Activity Comparison

A comparison of metabolic activity in a chemostat system and the BLP is shown in figure 4.6. The uninhibited methane consumption rates were measured in each system and compared.

The data shows that on a per mass basis the activity of the OB3b cells in the BLP system is about 25 times less than in the chemostat. This reduction is much more than would be expected from just diffusion inhibition of the alginate in the reactor. While this is a huge reduction in activity, the exact reason for this reduction has not yet been determined. One possibility is that the encapsulation process is inhibiting the cells in some way. While cellular viability of OB3b in the gel is high, something in the encapsulation process could be inhibiting cellular metabolism in the OB3b. One potential cause of inhibition could be the Ca^{2+} either held by the gel or from the initial crosslinking of the alginate causes MMO inhibition inside the cells. Another possibility is that the activity is reduced because the cells are very closely packed together in the gel. This may have some effect on the cells which slows their metabolism. Another possibility would be that the alginate structure does something mechanically to the cells to make them less active.

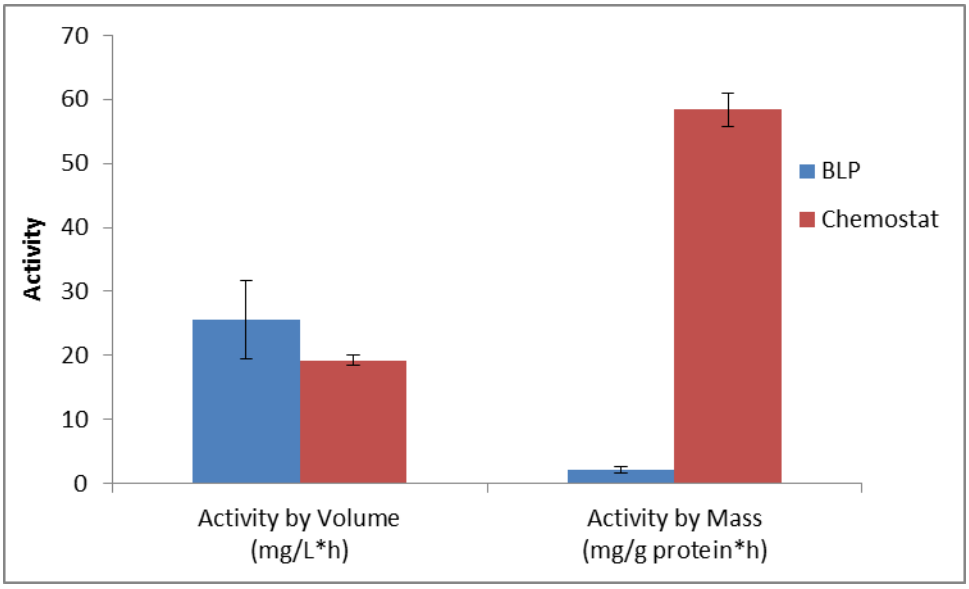

Figure 4. 6: A comparison of Chemostat and BLP activity based on volume and protein mass. Methane consumption rates of the BLP cells is shown to show the uninhibited activity of OB3b in each system. Error bars are based on a 95% confidence interval.

While the encapsulation process could be the cause of the reduced activity in the BLP, problems with the reactor itself could also be causing this reduction. The fluidics of the system have not been verified so it is possible that the reactor volume is not being fully utilized. One

concern with the system is that it was designed to be run at pressure with specific pressure drops in across the orifices at the inlet of the reactor. There has been some doubt that the flow and pressure controllers that have been fitted to the reactor are working as originally designed. If the pressures coming into the BLP are not regulated properly, then the flow distribution of the gasses throughout the reactor may not be ideal and gas bubbles may not be introduced across the entire width of the reactor. This would reduce the utilization of methane and oxygen in the reactor causing the average activity of the cells in the reactor to be reduced. Gel swelling could also be causing channeling of both gas and liquid flow in the reactor. This could cause flow maldistribution in the reactor which would prevent parts of the reactor from receiving nutrients. The BLP reactor has also been subject to fairly quick pressure changes. If the pressure rises to quickly it is possible that a significant number of cells will be damaged. If this were to happen then only a small number of cells would be alive to metabolize which would reduce the activity in the reactor. Further tests on the reactor fluidics and the activity of OB3b after cell encapsulation are needed in order to determine the exact cause of the reduced cellular activity.

This system is designed to maximize reactor performance on a per volume level. In this study the reactor performance in the BLP is not much better than in the chemostat. However, if the some of the problems with fluidics and potential reduced activity due to cell encapsulation are solved it is likely that the overall conversion in the BLP reactor will be significantly higher than the chemostat.

Methanol Production Performance in the BLP

Data from preliminary studies of methanol production in the BLP and chemostat systems are shown in figures 4.7 and 4.8. Figure 4.7 shows methanol production on a cell mass basis. The chemostat in these studies outperformed the BLP reactor in all experiments. The degree by which the chemostat outperformed the BLP was greater than expected. The alginate films in the BLP are

very thin so the mass transfer resistance of the substrate gases in the liquid media should be minimal. With these small diffusion lengths, it was expected that the cells in the BLP would show only a modest decrease in methanol production at worst, and potentially an increase in methanol production when compared to the chemostat if diffusion was the main consideration in the reactor. For this reason, it is not expected that diffusion resistance is the cause of decreased production and that it has something to do with reactor operation or some effect of the encapsulation of cells, such as those discussed at the end of the immobilized cell activity section. The exact reasons for this decrease are still under investigation.

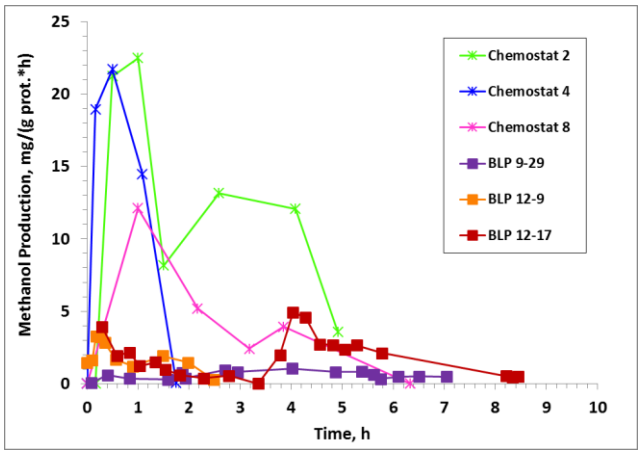

Figure 4. 7 Comparison of methanol production in the BLP and chemostat systems by cell mass.

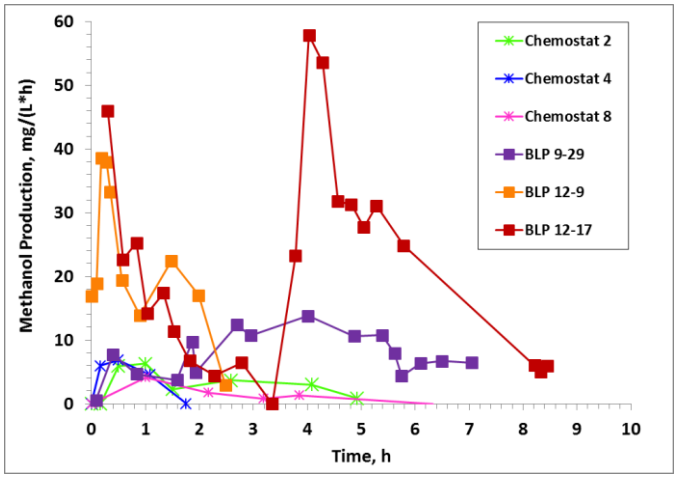

Figure 4. 8: Comparison of methanol production in the BLP and chemostat systems by reactor volume.

In figure 4.8, BLP and chemostat performance data on a volumetric basis are shown. In all instances, the methanol production in the BLP is higher than that of the chemostat. This data indicates that the BLP is capable of producing larger amounts of methanol in smaller systems than with other reactors. This was a main goal of the project and is a major step in reducing the size of gas to liquid reactors.

While the performance on a per volume basis is much better for the BLP it is still lower than our target goals for the project. The target methanol production for the project is 25 g methanol/(L-hr). Currently the methanol production in this system is about three orders of magnitude lower than these goals. There are a number of factors that could raise the methanol production rate of the reactor system to help us reach these goals. First of all the concentration of cells that were immobilized in the reactor in these experiments was 10-20 g cells/L. It is expected that cell concentrations up to 100 g/L or higher could be achieved in the BLP. The addition of more cells into the reactor could potentially help increase performance in the system 5-10 fold, if there is no detrimental effect of loading the cells in higher concentrations.

Another thing that could be done to improve reactor performance is to increase the pressure in the reactor. The reactor system was origionally designed to be operated at pressures of

20 bar. Operating the BLP at high pressure will significantly increase the amount of dissolved methane in the media of the reactor system. This will allow for higher methane fluxes through the media to the cells and also result in higher methane turnover rates for the OB3b. While pressurizing the reactor could help performance considerably, the viability of OB3b at these pressures has not been verified.

Optimizing the fluidics in the system could also be helpful to increase reactor performance. It is currently unknown how much of the reactor volume is being utilized. There is also evidence that in some of the tests media and gas bubbles are bypassing parts of the reactor. This would significantly reduce the performance of the reactor and improving flow distribution could significantly increase reactor performance.

Optimization of the inhibition of MDH also should to be done. Currently, cyclopropanol is added to the system in pulses and allowed to inhibit the reactor overnight. This allows the cells to regenerate the MDH over time which allows for the cells to replenish the electrons required for their metabolism. Further studies into the concentrations and exposure times of cyclopropanol to the system for maximum reactor performance should be performed. Also it may be beneficial to inhibit the reactor continuously with a low enough concentration of cyclopropanol such that MDH is not completely inhibited. This would allow the cells to metabolize a small amount of methanol in order to continuously replenish the electrons required in their metabolism while still allowing for some methanol accumulation.

While the amount of methanol that the BLP is producing is less than desired there is still room for improvement. It is currently unknown whether our performance goals can be reached, but with more optimization of the reactor it is likely that the reactor performance can be considerably improved.

Conclusions and Future Work

Studies as to whether or not the OB3b cells survive the gel encapsulation process have been performed. Both live/dead staining and metabolic tests in batch systems show that the cells are alive and capable of metabolizing. These tests indicate that there is a less than 10% loss of cells throughout the encapsulation process.

While the OB3b cells appear to be alive after the gel encapsulation process, it is possible that the cells have a reduced metabolism after the encapsulation process. Comparisons of methane consumption between the chemostat and BLP systems indicates that cellular activity in the BLP is lower than expected. This may be due to a loss of activity of the cells through the gel encapsulation process or it could be due to reactor performance. It is also possible that effects of the startup of the reactor system could affect the viability of the cells.

Preliminary data on the performance of the BLP shows that on a per mass basis methanol production in the BLP is lower than in the chemostat, but on a per volume basis the production rate is higher. This indicates that the BLP can produce greater amounts of methane in smaller volumes than free cell systems.

Currently the BLP is producing much less methanol than our target goal. Reactor performance could be increased through a number of changes including: increasing the number of cells in the reactor, increasing the pressure of the reactor, improving the fluidics of the reactor, and optimizing the MDH inhibition of the cells in the reactor.

A number of studies could be performed to better understand any metabolic problems with the cells in the reactor. Methane consumption studies should be performed with cells immobilized in thin alginate films. The flow cells described in chapter 2 would be an ideal system to test this. It is also worth testing whether there is a difference in methane consumption for cells immobilized using external gelation and internal gelation. Furthermore some studies should be

performed on whether or not the calcium used in the formation of the alginate affects MMO activity in OB3b.

Studies on the conditions of the cells after a BLP experiment could also be performed. This would help in the determination of whether a loss of cell activity in the reactor is caused by cell death or an inhibition of cellular function. These tests could be performed by using sodium citrate to dissolve the reactor gel after an experiment and test the cells for activity. Another method would be to do live/dead staining with a confocal microscope to observe cell lysis in the reactor. This would also make it possible to investigate the viability of cells at various depths in the reactor. This would provide insight on whether cells in the lower immobilized layers die from starvation or if cells die at other immobilized layers due to other causes.

Studies should also be performed to determine the best inhibition method for the cells in the reactor. Performing test with the continuous addition of low concentrations of cyclopropanol should be compared with tests where cyclopropanol is pulsed at higher concentrations. This could be done with the flow cells developed earlier which would allow for rapid testing of these inhibition conditions.

Ultimately, there is more work to be done with the BLP system itself. The fluidics of the system should be optimized to ensure proper substrate transport to all parts of the reactor. Studies on the volume utilization of the reactor should also be performed. Verification that the full controllers and pressure regulators are working to their designed specification also should be done and pressure fluctuations in the reactor system should be reduced or eliminated to prevent pressure spikes from harming the OB3b. If these problems are resolved it is likely that the performance of the BLP reactor will improve substantially.

Chapter 5

General Conclusions and Future Work

The work presented in this thesis offers insight into the immobilization of OB3b cells into a biolamina plate reactor (BLP). Immobilization of cells in this system is more-or-less unique application as the immobilization medium must be bound to the reactor surface, as opposed to beaded systems where the beads must be prevented from washing out of the reactor. This work discusses the challenges in immobilizing cells in this system, and several solutions for resolving these challenges. As the work on developing the BLP system is ongoing, this work also presents many recommendations for future studies and methods to improve reactor performance.

Successful encapsulation of methanotrophic OB3b cells in alginate hydrogels was achieved, and these hydrogels were adequately anchored to the reactor surface. In early experiments with phosphate media, the alginate hydrogels tended to swell and degrade in the reactor system. This caused obstruction of the liquid flow path in the reactor and caused reactor pressures to rise to unsustainable levels. A switch to HEPES buffered media in the reactor system seemed to substantially reduce the amount of gel degradation in the system, and allowed for successful reactor operation. This improvement is largely attributed to the removal of calcium-chelating phosphate in the media along with an increase in media buffering capacity. Further tests with microfluidic flow cells examined the conditions of alginate gels under flow with different media compositions and acidity. These tests verified that alginate gels performed better under HEPES buffered systems than phosphate buffered systems.

Alginate adhesion to the base of the reactor is another important aspect of cell immobilization in the reactor system. Early experiments indicated that simply adding microstructures on the BLP biofilm plates would not be adequate to anchor the alginate to the base of the reactor. It was found that proper cleaning and passivation of the reactor surface helped

alginate adhesion, but further adhesion strength was desirable to insure the gel did not slough from the surface. Chemical modification of stainless steel by APTMS provided better adhesion of the alginate to the surface. Experiments with this surface treatment indicated that it was adequate to anchor the alginate to the reactor through multiple experiments. Further testing showed that APTMS and polylysine coatings both provided increased adhesion strength of alginate to stainless steel. APTMS was chosen as the preferred reactor treatment due to its lower cost and potentially longer lasting effect on stainless steel. APTMS coatings were also validated on polycarbonate surfaces, which would enable future reactor designs to be made out of cheaper plastics.

OB3b cells have been shown to survive the encapsulation process with alginate. Both live/dead staining and batch metabolic tests indicate that OB3b cells remain intact and able to metabolize in alginate hydrogels. However, there is some indication that OB3b cells encapsulated in these gels have reduced ability to metabolize methane. This was evidenced by the difference in specific methane consumption rates of OB3b cells in the BLP and chemostat systems. This data is far from conclusive as problems with the fluidics and operation of the BLP system are still under investigation. Further studies are needed to determine whether alginate encapsulation of OB3b does in fact reduce its activity, or whether there are other causes for this phenomena relating to BLP operation.

Tests with the BLP system show that methanol can successfully be produced in the BLP. However the methanol production rates are low compared to targets that are required for economic feasibility. More work on the reactor system should be done to hit these targets. However, given that this reactor concept is still in its infancy, it is likely that further optimization of the system will result in greatly improved performance.

The knowledge gained from completing this work should be very valuable in moving forward to improve the system. Many suggestions for improved performance have been

`presented here with an extensive investigation of the causes of successes and failure of OB3b immobilization in the BLP thus far.

Bibliography

1. United States. Environmental Protection Agency. *Inventory of US Greenhouse Gas Emissions and Sinks: 1990-2013.* Environmental Protection Agency, 2015
2. United States. *Environmental Protection Agency. Summary Report: Global Anthropogenic Non-CO_2 Greenhouse Gas Emissions: 1990-2030.* Environmental Protection Agency, 2012
3. Strong, P. J., Sihuang Xie, and William P. Clarke. "Methane as a resource: can the methanotrophs add value?." *Environmental science & technology* 49.7 (2015): 4001-4018.
4. Showstack, R. (2015), *Initiative aims to end routine flaring of natural gas,* Eos, 96 (2015)
5. Ge, Xumeng, et al. "Biological conversion of methane to liquid fuels: status and opportunities." *Biotechnology Advances* 32.8 (2014): 1460-1475.
6. Haynes, Chad A., and Ramon Gonzalez. "Rethinking biological activation of methane and conversion to liquid fuels." *Nature chemical biology* 10.5 (2014): 331-339.
7. Velasco, Jorge A., et al. "Catalytic partial oxidation of methane over nickel and ruthenium based catalysts under low O 2/CH 4 ratios and with addition of steam." *Fuel* 153 (2015): 192-201.
8. Makarshin, L. L., et al. "Syngas production by partial oxidation of methane in a microchannel reactor over a Ni–Pt/La 0.2 Zr 0.4 Ce 0.4 O x catalyst." *Fuel Processing Technology* 131 (2015): 21-28.
9. Roberts, Ken. "Modular design of smaller-scale GTL plants." *Petroleum Technology Quarterly. Retrieved* (2013).
10. Periana, Roy A., et al. "Platinum catalysts for the high-yield oxidation of methane to a methanol derivative." *Science* 280.5363 (1998): 560-564.
11. Łojewska, Joanna, et al. "Promoting methane partial oxidation: homogenous additives impact on formaldehyde yield on vanadia catalyst." *Catalysis today* 101.2 (2005): 73-80.
12. Khirsariya, Priyank, and Raju K. Mewada. "Single Step Oxidation of Methane to Methanol–Towards Better Understanding." *Procedia Engineering* 51 (2013): 409-415.
13. Stokes, R, "Towards Zero routine flaring." *Petroleum Review* (2015): 38.
14. Fei, Qiang, et al. "Bioconversion of natural gas to liquid fuel: Opportunities and challenges." *Biotechnology Advances* 32.3 (2014): 596-614.
15. Mawatari, Kazuma, et al. "Microflow systems for chemical synthesis and analysis: approaches to full integration of chemical process." *Journal of Flow Chemistry* 1.1 (2012): 3-12.
16. Watts, Paul, and Charlotte Wiles. "Micro reactors, flow reactors and continuous flow synthesis." *Journal of Chemical Research* 36.4 (2012): 181-193.

17. Bieringer, Thomas, Sigurd Buchholz, and Norbert Kockmann. "Future Production Concepts in the Chemical Industry: Modular–Small-Scale–Continuous." *Chemical Engineering & Technology* 36.6 (2013): 900-910.
18. Hanson, Richard S., and Hanson, Thomas E.. "Methanotrophic bacteria." *Microbiological reviews* 60.2 (1996): 439-471.
19. Han, Ji-Sun, et al. "Partial oxidative conversion of methane to methanol through selective inhibition of methanol dehydrogenase in methanotrophic consortium from landfill cover soil." *Applied biochemistry and biotechnology* 171.6 (2013): 1487-1499.
20. Han, Ji-Sun, et al. "Partial oxidative conversion of methane to methanol through selective inhibition of methanol dehydrogenase in methanotrophic consortium from landfill cover soil." *Applied biochemistry and biotechnology* 171.6 (2013): 1487-1499.
21. Sirajuddin, Sarah, and Amy C. Rosenzweig. "Enzymatic oxidation of methane." *Biochemistry* 54.14 (2015): 2283-2294.
22. Sugimori, Daisuke, Masayuki Takeguchi, and Ichiro Okura. "Biocatalytic methanol production from methane with Methylosinus trichosporium OB3b: an approach to improve methanol accumulation." *Biotechnology letters* 17.8 (1995): 783-784.
23. Lee, Sung-Woo, et al. "Mixed pollutant degradation by Methylosinus trichosporium OB3b expressing either soluble or particulate methane monooxygenase: can the tortoise beat the hare?." *Applied and environmental microbiology* 72.12 (2006): 7503-7509.
24. Groboillot, A. F., et al. "Membrane formation by interfacial cross-linking of chitosan for microencapsulation of Lactococcus lactis." *Biotechnology and bioengineering* 42.10 (1993): 1157-1163.
25. Cadic, Ch, et al. "In vitro culture of hybridoma cells in agarose beads producing antibody secretion for two weeks." *Biotechnology and bioengineering* 39.1 (1992): 108-112.
26. Muthukumarasamy, Parthiban, Paula Allan-Wojtas, and Richard A. Holley. "Stability of Lactobacillus reuteri in different types of microcapsules." *Journal of Food Science* 71.1 (2006): M20-M24.
27. Rialland, L., et al. "Viability and drug metabolism capacity of alginate-entrapped hepatocytes after cryopreservation." *Cell biology and toxicology* 16.2 (2000): 105-116.
28. Murtas, S., et al. "Alginate beads as immobilization matrix for hepatocytes perfused in a bioreactor: a physico-chemical characterization." *Journal of Biomaterials Science, Polymer Edition* 16.7 (2005): 829-846.
29. Lee, Kuen Yong, et al. "Controlling mechanical and swelling properties of alginate hydrogels independently by cross-linker type and cross-linking density." *Macromolecules* 33.11 (2000): 4291-4294.
30. LeRoux, Michelle A., Farshid Guilak, and Lori A. Setton. "Compressive and shear properties of alginate gel: effects of sodium ions and alginate

concentration." *Journal of biomedical materials research* 47.1 (1999): 46-53.
31. Whistler, Roy, and James BeMiller. "Carbohydrate chemistry for food scientists." (2008): 146-146.
32. Kong, Hyun Joon, Molly K. Smith, and David J. Mooney. "Designing alginate hydrogels to maintain viability of immobilized cells." *Biomaterials* 24.22 (2003): 4023-4029.
33. Serp, D., et al. "Characterization of an encapsulation device for the production of monodisperse alginate beads for cell immobilization." *Biotechnology and bioengineering* 70.1 (2000): 41-53.
34. Lee, Christopher SD, et al. "Regulating in vivo calcification of alginate microbeads." *Biomaterials* 31.18 (2010): 4926-4934.
35. Haug, A. R. N. E., Björn Larsen, and Olav Smidsrød. "The degradation of alginates at different pH values." *Acta Chem Scand* 17.5 (1963): 1466-68.
36. Kuo, Catherine K., and Peter X. Ma. "Ionically crosslinked alginate hydrogels as scaffolds for tissue engineering: part 1. Structure, gelation rate and mechanical properties." *Biomaterials* 22.6 (2001): 511-521.
37. Kim, Bum Jin, et al. "Mussel-Mimetic Protein-Based Adhesive Hydrogel." *Biomacromolecules* 15.5 (2014): 1579-1585.
38. Hou, Junxia, et al. "Enzymatically crosslinked alginate hydrogels with improved adhesion properties." *Polymer Chemistry* (2015).
39. Palacio, Manuel LB, and Bharat Bhushan. "Bioadhesion: a review of concepts and applications." *Philosophical Transactions of the Royal Society A: Mathematical, Physical and Engineering Sciences* 370.1967 (2012): 2321-2347.
40. Chuang, T-W., M-H. Chen, and F-H. Lin. "Preparation and surface characterization of HMDI-activated 316L stainless steel for coronary artery stents." *Journal of Biomedical Materials Research Part A* 85.3 (2008): 722-730.
41. ASTM Standard D1002, 2010, "Standard Test Method for Apparent Shear Strength of Single-Lap-Joint Adhesively Bonded Metal Specimens by Tension Loading (Metal-to-Metal)", ASTM International, West Conshohocken, PA, 2010, DOI: 10.1520/D1002-10, www.astm.org
42. Zhu, Mojun, Maria Z. Lerum, and Wei Chen. "How to prepare reproducible, homogeneous, and hydrolytically stable aminosilane-derived layers on silica." *Langmuir* 28.1 (2011): 416-423.
43. Howarter, John A., and Jeffrey P. Youngblood. "Surface modification of polymers with 3-aminopropyltriethoxysilane as a general pretreatment for controlled wettability." *Macromolecules* 40.4 (2007): 1128-1132.
44. Jang, Minjeong, Chan Kyung Park, and Nae Yoon Lee. "Modification of polycarbonate with hydrophilic/hydrophobic coatings for the fabrication of microdevices." *Sensors and Actuators B: Chemical* 193 (2014): 599-607.

45. Gao, Hong, et al. "Preparation and properties of microencapsulated genetically engineered bacteria cells for oral therapy of uremia." *Chinese Science Bulletin* 49.11 (2004): 1117-1121.

APPENDICES

APPENDIX A

Schematics of Flow Cells

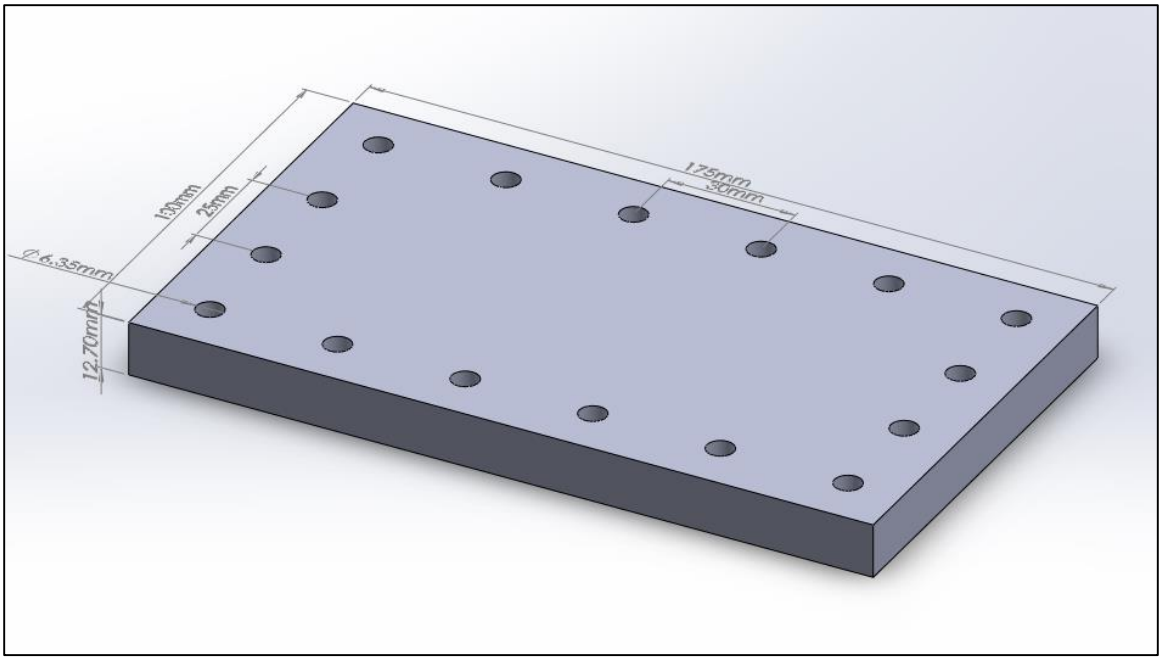

Figure A. 1: SolidWorks drawing of the PC flow cell top piece.

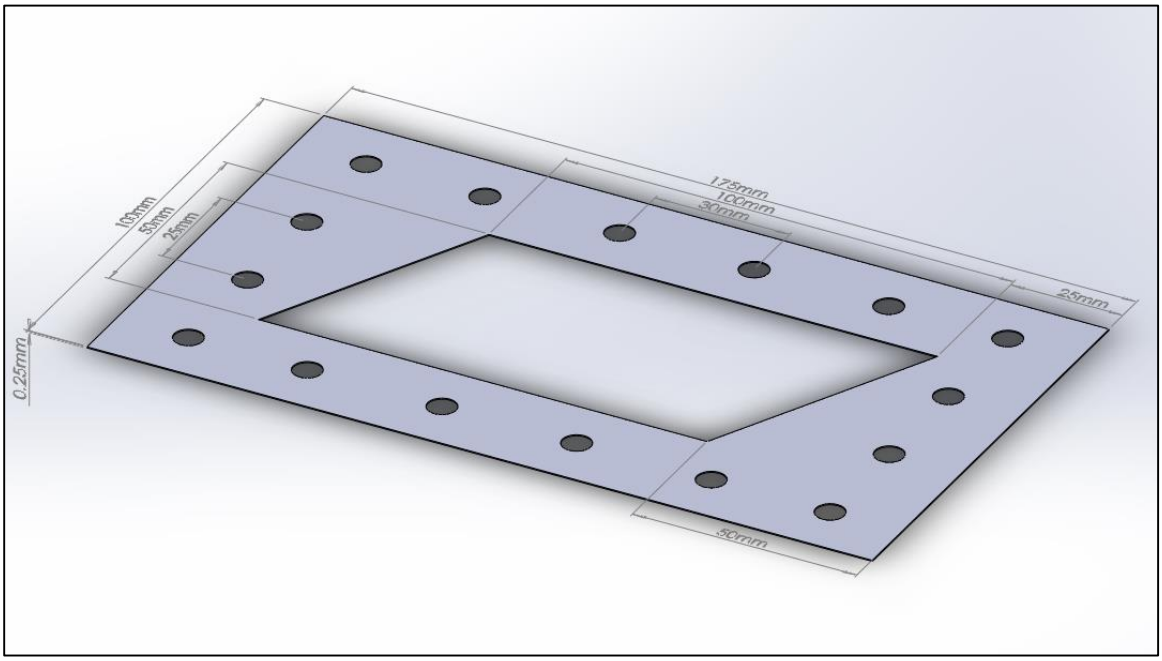

Figure A. 2: SolidWorks drawing of the PEEK flow spacer. Two spacers are used in each flow cell.

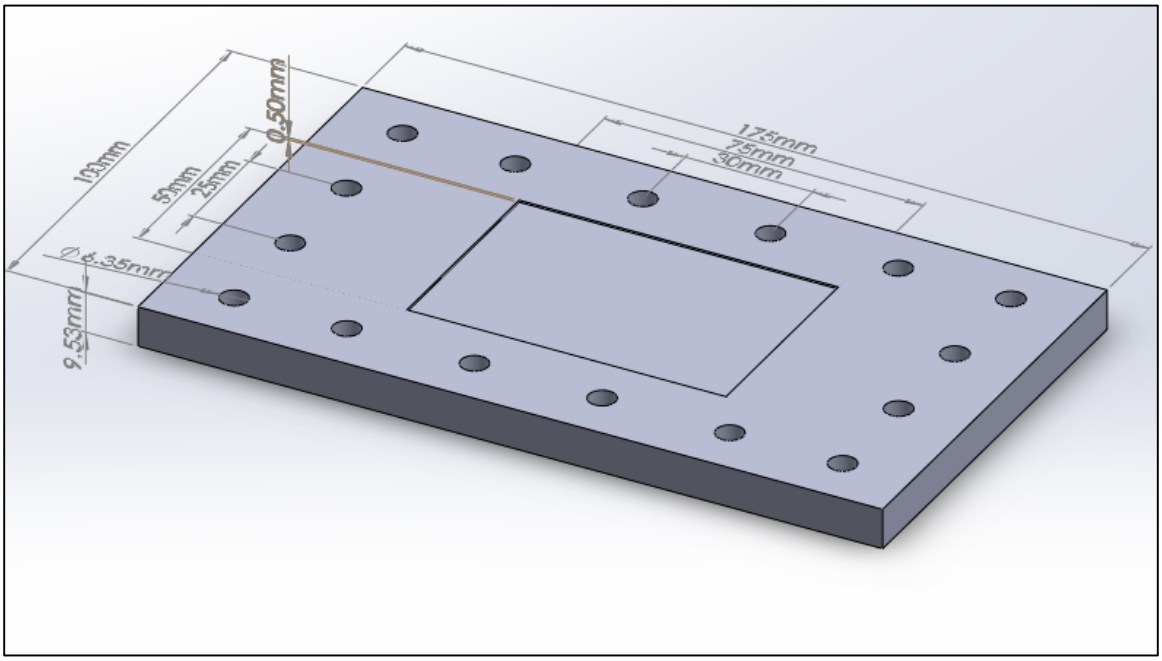

Figure A. 3: SolidWorks drawing of the PC flow cell base plate.

APPENDIX B

Live Dead Staining Controls

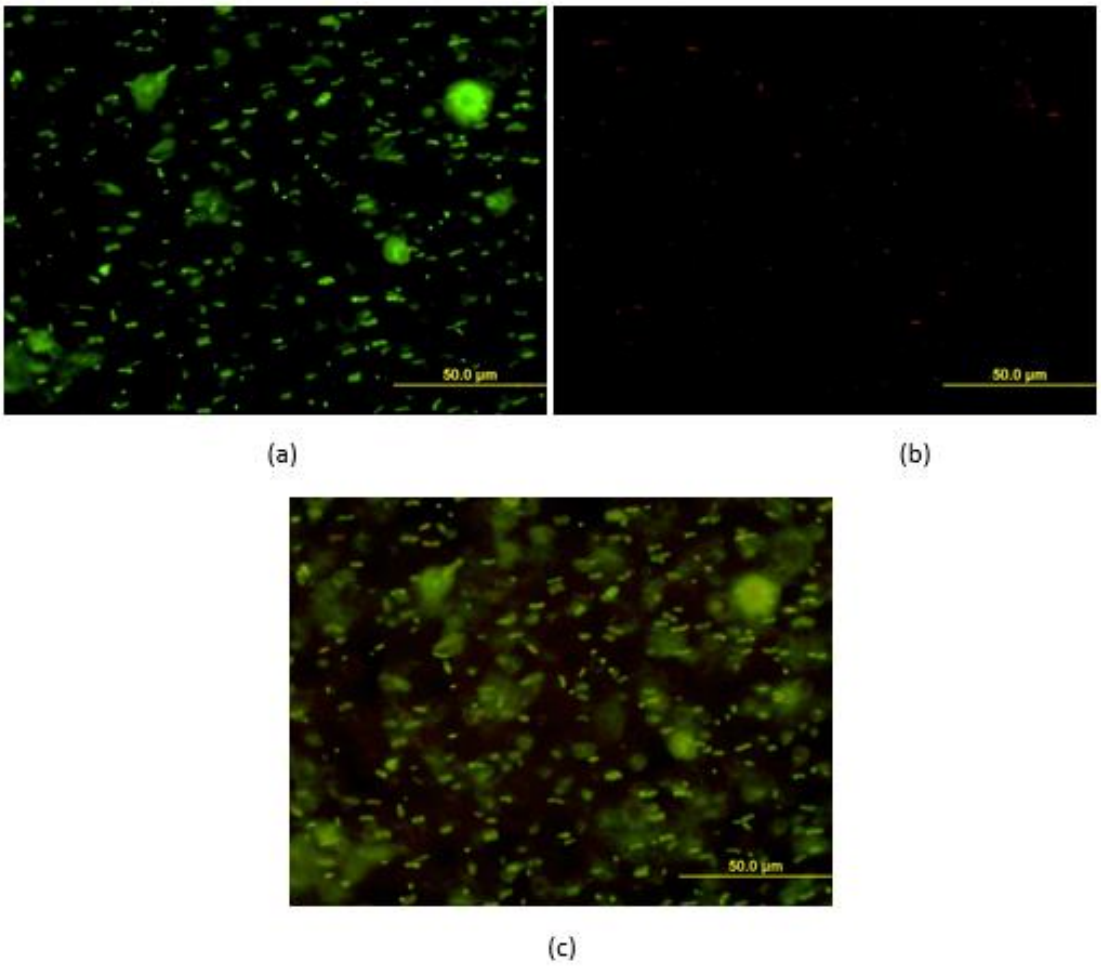

Figure B. 1: Live/Dead staining of OB3b cells in PBS. (a) shows the cells under a GFP filter, (b) under a Texas Red filter, and (c) under a longpass filter. A comparison of pictures (a) and (b) indicates that the vast majority of cells in the solution are live, with minimal dead cells

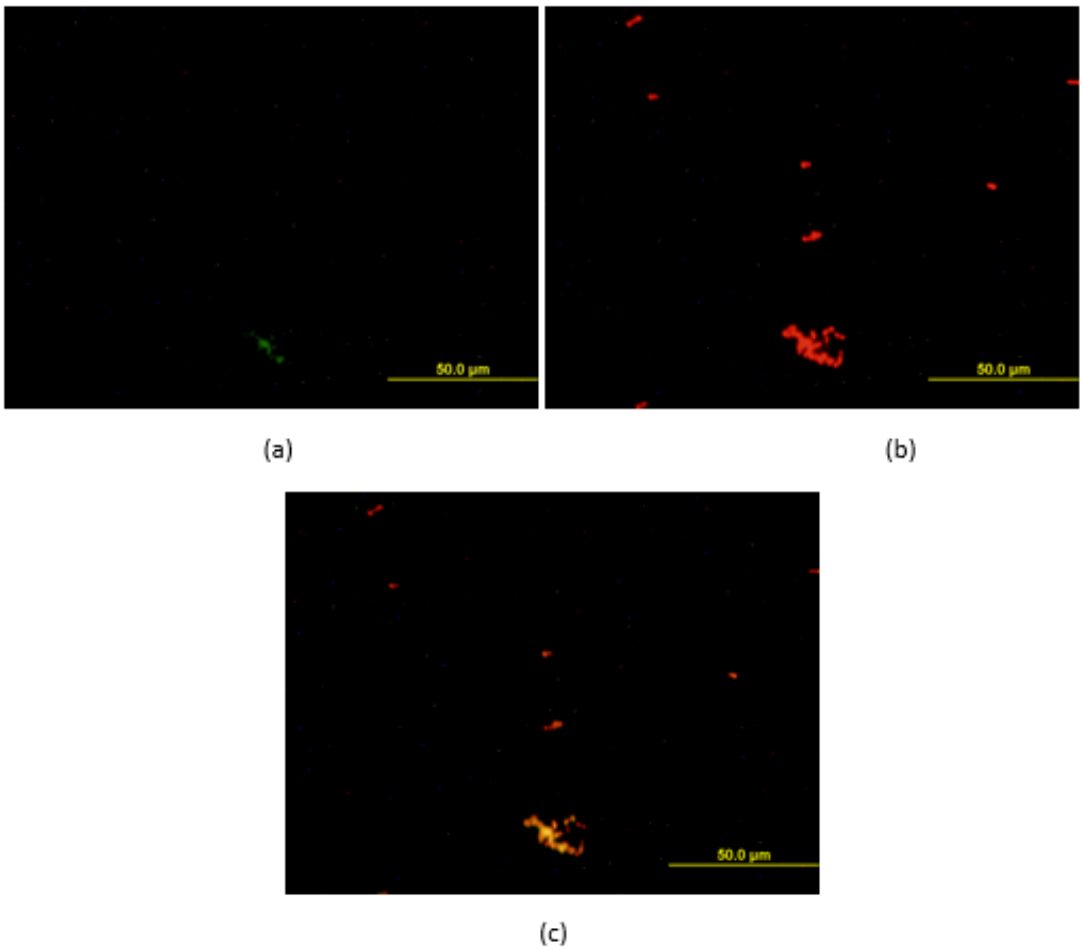

Figure B. 2: Live/Dead staining of OB3b cells in PBS after lysis with 70% ethanol. (a) shows the cells under a GFP filter, (b) under a Texas Red filter, and (c) under a longpass filter. Analysis of figures (a) and (b) shows all the cells in the control to be dead.

APPENDIX C

Media Formulations

Phosphate Media

Part A	Mix in 1 L water:		
g	Component	stock solution concentration	volume of stock per L
1	KNO_3	25g/100ml	4 ml
1	$MgSO_4 \cdot 7\ H_2O$	25g/100ml	4 ml
0.134	$CaCl2 \cdot\ H_2O$	13.4g/100ml	1 ml
0.025	KH_2PO_4	2.5g/100ml	1 ml

Autoclave Part A
When Part A has returned to room temp add Parts B and C which have been autoclaved, and cooled, separately

Part B			
g	Component	stock solution concentration	volume of stock per L
0.7	$Na_2HPO_4 \cdot 7\ H_2O$	7g/100ml	10 ml

Part C	
2 ml trace elements solution	
Mix in 1 L of water:	
g	Component
1.29	Na_2EDTA
1.69	$FeSO_4 \cdot 7\ H_2O$
0.8	$ZnSO_4 \cdot 7\ H_2O$
0.005	$MnCl_2 \cdot 2\ H_2O$
0.03	H_3BO_3
0.05	$CoCl_2 \cdot 6\ H_2O$
0.002	$NiCl_2 \cdot 6\ H_2O$
0.05	$Na_2MoO_4 \cdot 2\ H_2O$

HEPES Media

Part A	Mix in 1 L water:		
g	Component	stock solution concentration	volume of stock per L
1	KNO_3	25g/100ml	4 ml
1	$MgSO_4 \cdot 7\ H_2O$	25g/100ml	4 ml
0.134	$CaCl2 \cdot\ H_2O$	13.4g/100ml	1 ml

Autoclave Part A
When Part A has returned to room temp add Parts B and C which have been autoclaved, and cooled, separately

Part B	
g	Component
2.4	HEPES

Part C	
2 ml trace elements solution	
Mix in 1 L of water:	
g	Component
1.29	Na_2EDTA
1.69	$FeSO_4 \cdot 7\ H_2O$
0.8	$ZnSO_4 \cdot 7\ H_2O$
0.005	$MnCl_2 \cdot 2\ H_2O$
0.03	H_3BO_3
0.05	$CoCl_2 \cdot 6\ H_2O$
0.002	$NiCl_2 \cdot 6\ H_2O$
0.05	$Na_2MoO_4 \cdot 2\ H_2O$

APPENDIX D

Summary of Reactor Experiments

(Starts on next page)

Table D.1: Summary of BLP experiment tests

Experiment #	Date	Description	Phases	Flow Rates [ml/min]	Initial Pressures [psi]	Final Pressures [psi]	Effluent Condition	Notes/Observations/Learnings
1	20-Aug-14	Gas Pressure Test	Gas only		$P_{H2O,in}$=290 P_{out}=285			No leaks Solenoid valves started to tick
	21-Aug-14	Gas Pressure Test II	Gas	~75	P_{gas}=491 P_{in}=292 P_{out}=288			No Leaks Solenoids started knocking after about 30 mins. By passed them.
	21-Aug-14	Gas Pressure Test III (added water)	Gas & Liquid	H2O ~ 11 Gas ~110	P_{gas}=612 P_{H2O}=307 P_{H2Oin}=292 P_{out}=272			No leaks
	21-Aug-14	Gas Pressure Test IV (turned off water)	Gas	~42 to 115	P_{gas}=336 P_{in}=294 P_{out}=286	P_{gas}=510 P_{in}=294 P_{out}=286		Gas flow rates and pressure drop across reactor remained stable.
2	22-Aug-14	Gel, gas only (tried to add water later)	Gas w/Gel		P_{gas}=100 P_{in}=17 P_{out}=0	P_{gas}=250 P_{in}=24 P_{out}=0		Took an hour to stabilize at each pressure levels Flow rate increased from 1 ml/min to 5 ml/min Turned on water but was not able to get any liquid flow. Plates damaged?

Table D.1: Summary of BLP experiment tests (continued)

3	29-Aug-14	Gel pressure check	Liquid only					Only H_2O seeing a 100 psi drop across the reactor Plates damaged/clogged. Ultrasonic'd plate and tried again, same problem. Plates damaged?
4	3-Sep-14	No Gas Holes Plate I	Liquid & Gas	5.7	P_{H2O}=75 P_{H2Oin}=53 P_{out}=16	P_{gas}=67 P_{H2O}=61 P_{H2Oin}=36 P_{out}=30		Gas added into liquid feed line
	3-Sep-14	No Gas Holes Plate II	Liquid	5.7-7.6	P_{H2O}=32 P_{H2Oin}=10 P_{out}=9	P_{H2O}=34 P_{H2Oin}=10 P_{out}=9		Running gel plate upside down (can it simulate gel?)
	3-Sep-14	No Gas Holes Plate III	Liquid & Gas	Liq 7.6 Gas 67	P_{H2O}=34 P_{H2Oin}=10 P_{out}=9	P_{gas}=70 P_{H2O}=44 P_{H2Oin}=21 P_{out}=20		Running gel plate upside down (can it simulate gel?) Gas added into liquid feed line
5	5-Sept-14	No Gas Holes w/Gel	Liquid & Gas	Liq 5.7-9.5 Gas 0-230	P_{H2O}=34 P_{H2Oin}=11 P_{out}=10	P_{gas}=66 P_{H2O}=53 P_{H2Oin}=29 P_{out}=29		Testing gel integrity. First ran with only H2O then added air into H2O stream. Ran air flow up to 230 ml/min
6	17-Sep-14 20-Sep-14	First OB3b in reactor	Liquid & Gas	Liq 0.8-1.5 Gas 0-22	P_{air}=36 P_{CH4}=0 P_{H2O}=33 P_{H2Oin}=14 P_{out}=13	P_{air}=124 P_{CH4}=43 P_{H2O}=58 P_{H2Oin}=38 P_{out}=38		No Gas Holes Plate, $1/10^{th}$ media By passed pressure regulator and exit filter (pressure out drop down to atm) Ran over multiple days Inhibited on day 3 over lunch

Table D.1: Summary of BLP experiment tests (continued)

7	25-Sep-14 30-Sep-14	New Top Plate	Liquid, Gas & Gel	Liq 1.5-0.7 Gas nm	P_{air}=23 P_{CH4}=25 P_{H2O}=28 P_{H2Oin}=6 P_{out}=1	P_{air}=13 P_{CH4}=17 P_{H2O}=26 P_{H2Oin}=8 P_{out}=0		First day was liquid and gas, inhibited over night with cPOH using syringe pump 27^{TH} added formate Left gel in reactor over weekend w/ CH4/O2 infused media
8	24-Oct-14 31-Oct-14	Internal Gel CH4/O2 infused media	Liquid, Gas & Gel	Liq 0.5-0.06 Then 0.2	P_{H2Oin}=7 P_{out}=0	P_{H2O}=20 P_{H2Oin}=4 P_{out}=0		Ran w/ CH4/O2 infused media w/ syringe pump 24^{th} inhibited over night with cPOH. 28^{th} flowed ~ 2 ml of 100 μm $CaCl_4$ 29^{th} put on cPOH, w/ HPLC pressure in reactor was too high for syringe pump, switch back to HPLC but still infused
9	10-Nov-14 12-Nov-14	Gel stability test	Liquid & Gel	Liq 0.5	P_{H2Oin}=2 P_{out}=0	P_{H2Oin}=3 P_{out}=0		Gel (no bugs) long term run to see why it melted before using $1/10^{th}$ media (w/ right amount to Ca) 11^{th} turned off HPLC to swap bottles

Table D.1: Summary of BLP experiment tests (continued)

10	19-Nov-14 26-Nov-14	Gel w/ OB3b stability test	Infused Liquid & Gel	Liq 0.5-4.0	P_{H2Oin}=1 P_{out}=0	P_{H2Oin}=19 P_{out}=0	Effluent pH range 5.8-7.1 Influ 7.6	Feeding 1/10th media infused w/ CH4/O2 & gas bag attached to bottle
11	9-Dec-14 12-Dec-14	Gel w/ OB3b	Infused Liquid & Gel	Liq 0.5-4.0	P_{H2Oin}=2 P_{out}=0	P_{H2Oin}=21 P_{out}=0	Effluent pH range 6.8-7.3 Influ 7.5	Feeding 1/10th media infused w/ CH4/O2 & gas bag attached to bottle 10th swapped at end of day but forgot to open it. DO_{in}=48%, DO_{ef}=9% 10th inhibited w/ cPOH over lunch
12	17-Dec-14 19-Dec-14	External Gel w/ OB3b (10.6 g)	Infused Liquid & Gel Gas later	Liq 2.0	P_{H2O}=28 to 43 P_{H2Oin}=5 P_{out}=0	P_{air}=146 P_{CH4}=126 P_{H2O}=45 P_{H2Oin}=6 P_{out}=0	Effluent pH range 7.2-7.4 Influ 7.6	Feeding 1/10th media infused w/ CH4/O2 & gas bag attached to bottle 18th inhibited w/ cPOH over night HPLC leaking ~ ¼ ml/min

Table D.1: Summary of BLP experiment tests (continued)

13	21-Jan-15 28-Jan-15	Flow Test w/ Acrylic Gel/Clamp Plate	Liquid & Gas (plate acts as gel)	Liq 2-4.0	P_{H2Oin}=15 P_{out}=0	$P_{gas,in}$=79 P_{H2Oin}=54 P_{out}=0		Leaking. After adding Teflon tape to bolts & torque equal to steel plate, still leaking Noticed some of the gas was flowing backwards out of bow ties and then was using the O-ring groove to flow to the exit port. Acrylic was defecting (build frame) Steel marked acrylic